J|A|C|S ARTICLES

Published on Web 09/15/2009

EPR and ENDOR Characterization of the Reactive Intermediates in the Generation of NO by Cryoreduced Oxy-Nitric Oxide Synthase from *Geobacillus stearothermophilus*§

Roman Davydov,† Jawahar Sudhamsu,‡ Nicholas S. Lees,† Brian R. Crane,*,‡ and Brian M. Hoffman*,†

Chemistry Department, Northwestern University, Evanston, Illinois 60208-3113, and Department of Chemistry and Chemical Biology, Cornell University, Ithaca, New York 14853-1301

Received July 22, 2009; E-mail: bc69@cornell.edu; bmh@northwestern.edu

Abstract: Cryoreduction EPR/ENDOR/step-annealing measurements with substrate complexes of oxy-gsNOS (**3**; gsNOS is nitric oxide synthase from *Geobacillus stearothermophilus*) confirm that Compound I (**6**) is the reactive heme species that carries out the gsNOS-catalyzed (Stage I) oxidation of L-arginine to *N*-hydroxy-L-arginine (NOHA), whereas the active species in the (Stage II) oxidation of NOHA to citrulline and HNO/NO^- is the hydroperoxy-ferric form (**5**). When **3** is reduced by tetrahydrobiopterin (BH4), instead of an externally supplied electron, the resulting $BH4^+$ radical oxidizes HNO/NO^- to NO. In this report, radiolytic one-electron reduction of **3** and its complexes with Arg, Me-Arg, and NO_2Arg was shown by EPR and ^{1}H and ^{14,15}N ENDOR spectroscopies to generate **5**; in contrast, during cryoreduction of **3**/NOHA, the peroxo-ferric-gsNOS intermediate (**4**/NOHA) was trapped. During annealing at 145 K, ENDOR shows that **5**/Arg and **5**/Me-Arg (but not **5**/NO_2Arg) generate a Stage I primary product species in which the OH group of the hydroxylated substrate is coordinated to Fe(III), characteristic of **6** as the active heme center. Analysis shows that hydroxylation of Arg and Me-Arg is quantitative. Annealing of **4**/NOHA at 160 K converts it first to **5**/NOHA and then to the Stage II primary enzymatic product. The latter contains Fe(III) coordinated by water, characteristic of **5** as the active heme center. It further contains quantitative amounts of citrulline and HNO/NO^-; the latter reacts with the ferriheme to form the NO-ferroheme upon further annealing. Stage I delivery of the first proton of catalysis to the (unobserved) **4** formed by cryoreduction of **3** involves a bound water that may convey a proton from L-Arg, while the second proton likely derives from the carboxyl side chain of Glu 248 or the heme carboxylates; the process also involves proton delivery by water(s). In the Stage II oxidation of NOHA, the proton that converts **4**/NOHA to **5**/NOHA likely is derived from NOHA itself, a conclusion supported by the pH invariance of the process. The present results illustrate how the substrate itself modulates the nature and reactivity of intermediates along the monooxygenase reaction pathway.

Nitric oxide plays an essential role in many biological processes. In mammals, these include vasodilation, neurotransmission, and immune responses.[1−6] In eukaryotes, NO is mainly synthesized by nitric oxide synthase (NOS), which catalyzes the O_2-dependent conversion of L-arginine to L-citrulline and NO via two consecutive reactions, with N^{ω}-hydroxy-L-arginine (NOHA) as a stable intermediate (eq 1).[2,7−9] Mammalian NOSs

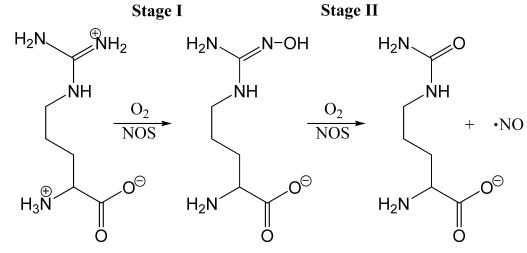

(1)

are homodimeric, with each subunit containing a reductase domain (NOS_{red}), which binds flavin adenine dinucleotide (FAD), flavin mononucleotide (FMN), and the reduced form of nicotinamide adenine dinucleotide phosphate (NADPH), and an oxygenase domain (NOS_{ox}), which binds heme, substrate, and an essential tetrahydropterin cofactor (BH4). A calmodulin binding region intervenes between the two domains and regulates reduction of NOS_{ox} by NOS_{red} in response to Ca^{2+}-

† Northwestern University.
‡ Cornell University.
§ Abbreviations used: NOS, nitric oxide synthase; e-, i-, and nNOS, endothelial, inducible, and neuronal NOSs; gsNOS, NOS from *Geobacillus stearothermophilus*; bsNOS, NOS from *Bacillus subtilis*; NOS_{ox}, oxidase domain of NOS; NOS_{red}, reductase domain of NOS; Arg, L-arginine; NOHA, N^{ω}-hydroxy-L-arginine; Me-Arg, N^{ω}-methyl-L-arginine; NO_2Arg, N^{ω}-NO_2-L-arginine; Cpd I, Compound I; sf, substrate-free; BH4, tetrahydrobiopterin.

(1) Bruckdorfer, R. *Mol. Aspects Med.* **2005**, *26*, 3–31.
(2) Alderton, W. K.; Cooper, C. E.; Knowles, R. G. *Biochem. J.* **2001**, *357*, 593–615.
(3) Barbato, J. E.; Tzeng, E. *J. Vasc. Surg.* **2004**, *40*, 187–193.
(4) Nott, A.; Riccio, A. *Cell Cycle* **2009**, *8*, 725–730.
(5) Pfeiffer, S.; Mayer, B.; Hemmens, B. *Angew. Chem., Int. Ed.* **1999**, *38*, 1715–1731.
(6) Yun, H. Y.; Dawson, V. L.; Dawson, T. M. *Mol. Psychiatry* **1997**, *2*, 300–310.

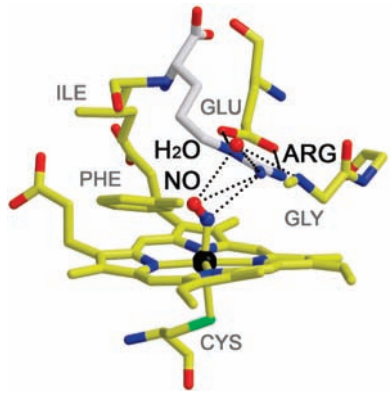

Figure 1. Active center of *B. subtilis* NO-ferro-bsNOS/L-arginine (PDB code 2FC1); residue composition of the *B. subtilis* NOS active site is identical to that of gsNOS.[12]

binding. During catalysis, electrons transfer from NADPH through FAD and FMN in NOS_{red} of one subunit of the homodimer to the NOS_{ox} of the other subunit.

Crystal structures of the oxygenase domains of mammalian NOSs show a distinct protein fold in which the heme is coordinated by a cysteine residue on the proximal side, as in cytochromes P450. Substrate Arg and intermediate NOHA both bind in a similar configuration above the heme iron atom in the distal pocket. BH4 binds at the dimer interface, with a heme propionate directly interacting with the 3,4 amide moiety of the pterin ring. BH4 has the critical role of rapidly supplying an electron to the heme-oxy species in both steps of catalysis.[8] In the resting state of NOS the heme is a mixture of five- and six-coordinate species, with water as the sixth axial ligand. Substrate binding converts the heme center completely to the five-coordinate, high-spin $S = 5/2$ configuration.

NOS homologues have been identified in a number of mostly Gram-positive bacterial species.[10] In particular, a thermostable NOS-like protein from the thermophilic bacterium *Geobacillus stearothermophilus* (gsNOS) has been isolated and studied.[11] This bacterial NOS is similar to the oxygenase domain of mammalian NOSs but contains no associated reductase domain.[11] Reductase partners for gsNOS are yet to be identified, but bacterial flavodoxins can act as efficient electron donors to closely related bacterial NOSs.[10] gsNOS successfully oxidizes arginine to NO by O_2 in single-turnover studies *in vitro* if provided with a mammalian NOS_{red} domain and BH4.[11] The crystal structures of bacterial NOSs are very similar to that of mammalian NOS_{ox}, with the exception of some subtle changes in the distal heme pocket that may be related to the enhanced ligand stability. Figure 1 shows the active site of an analogue for **3**, NO-ferro-NOS from *Bacillus subtilis*, with Arg held adjacent to the bound diatomic, along with a bound water at or near H-bonding distance from NO and the guanidinium group of Arg (PDB code 2FC1; residue composition of the *B. subtilis* NOS active site is identical to that of gsNOS).[12]

O_2 activation by heme monooxygenases such as the P450s, heme oxygenase (HO), and NOSs including gsNOS is understood in terms of a sequence of reactions, beginning with reduction of the ferriheme (**1**) to ferroheme (**2**) by the NADPH reductase domain, O_2 binding to form the oxy-ferroheme (**3**), and then one-electron reduction to form the peroxo-ferriheme (**4**), as depicted in Scheme 1. State **4** can react with the substrate to form a primary product (**7**), or it can accept a proton to generate the hydroperoxo-ferric state (**5**). Note that species **4** and **5** can be resolved only upon reduction of **3** at 77 K by radiolytically generated electrons.[13] Under physiological conditions, or in the presence of electron donors with positive redox potentials, formation of species **5** likely occurs via proton-coupled electron transfer to **3**.[14] If species **5** does form, it in turn can react with substrate to form product **7** or accept a second proton, generating Compound I (Cpd I; **6**), the most reactive of the three possible reactive forms, which would then react with substrate. In the reaction of mammalian NOSs with L-Arg, BH4 provides the electron that reduces **3**, and the resulting BH4 radical is reduced by the reductase domain, while in the reaction with NOHA the BH4 radical probably is reduced by NO^- or the Fe(II)NO complex.[15,16]

A central task in the study of every heme monooxygenation reaction is the determination of the reactive heme species that transforms substrate: **4**, **5**, or **6**. It is widely held that the Stage I conversion of L-Arg to NOHA involves a cytochrome P450-type monooxygenation by the high-valent iron-oxo species (**6**) as the catalytically active intermediate,[7,8] while the peroxy (**4**) or hydroperoxy species (**5**) is proposed to carry out the Stage II conversion of NOHA to citrulline plus NO.[17] However, bacterial NOSs, horseradish peroxidase, and some resin-supported Fe(III) porphyrins are efficient catalysts for H_2O_2-mediated oxidation of L-Arg to citrulline and NO, possibly by action of **6**.[11,18−20] This is further supported by recent DFT computations that suggested Cpd I (**6**) could also be acting as the reactive species in the oxidation of NOHA.[21] Finally, it was also shown[7,20] that NOSs not only catalyze the O_2-dependent oxidation of NOHA to NO and citrulline but also exhibit an alternate reaction that generates cyanoornithine and HNO as products when hydrogen peroxide is the oxidant.

Reactive intermediates **4**−**6** have largely evaded detection under physiological conditions because all are much shorter-lived than the oxy complex **3**. A notable exception is the recent observation of a kinetically competent, presumed ferryl species formed by a NOS_{ox} variant, in which hydrogen-bonding to the proximal Cys has been altered by a Trp-to-His substitution.[22] However, application of cryoreduction in combination with advanced EPR spectroscopy has enabled the characterization

(7) Marletta, M. A.; Hurshman, A. R.; Rusche, K. M. *Curr. Opin. Chem. Biol.* **1998**, *2*, 656–663.
(8) Stuehr, D. J.; Santolini, J.; Wang, Z.-Q.; Wei, C.-C.; Adak, S. *J. Biol. Chem.* **2004**, *279*, 36167–36170.
(9) Zhu, Y.; Silverman, R. B. *Biochemistry* **2008**, *47*, 2231–2243.
(10) Sudhamsu, J.; Crane, B. R. *Trends Microbiol.* **2009**, *17*, 212–218.
(11) Sudhamsu, J.; Crane, B. R. *J. Biol. Chem.* **2006**, *281*, 9623–9632.
(12) Pant, K.; Crane, B. R. *Biochemistry* **2006**, *45*, 2537–2544.
(13) Davydov, R.; Makris, T. M.; Kofman, V.; Werst, D. W.; Sligar, S. G.; Hoffman, B. M. *J. Am. Chem. Soc.* **2001**, *123*, 1403–1415.
(14) Cho, K.-B.; Carvajal, M. A.; Shaik, S. *J. Phys. Chem. B* **2009**, *113*, 336–346.
(15) Wei, C.-C.; Wang, Z.-Q.; Hemann, C.; Hille, R.; Stuehr, D. J. *J. Biol. Chem.* **2003**, *278*, 46668–46673.
(16) Stuehr, D. J.; Wei, C.-C.; Wang, Z.; Hille, R. *Dalton Trans.* **2005**, 3427–3435.
(17) Woodward, J. J.; Chang, M. M.; Martin, N. I.; Marletta, M. A. *J. Am. Chem. Soc.* **2009**, *131*, 297–305.
(18) Cai, T.; Xian, M.; Wang, P. G. *Bioorg. Med. Chem. Lett.* **2002**, *12*, 1507–1510.
(19) Mukherjee, M.; Ray, A. R. *Catal. Commun.* **2007**, *8*, 1431–1437.
(20) Clague, M. A.; Wishnok, J. S.; Marletta, M. A. *Biochemistry* **1997**, *36*, 14465–14473.
(21) Robinet, J. J.; Cho, K.-B.; Gauld, J. W. *J. Am. Chem. Soc.* **2008**, *130*, 3328–3334.
(22) Tejero, J.; Biswas, A.; Wang, Z.-Q.; Page, R. C.; Haque, M. M.; Hemann, C.; Zweier, J. L.; Misra, S.; Stuehr, D. J. *J. Biol. Chem.* **2008**, *283*, 33498–33507.

Scheme 1

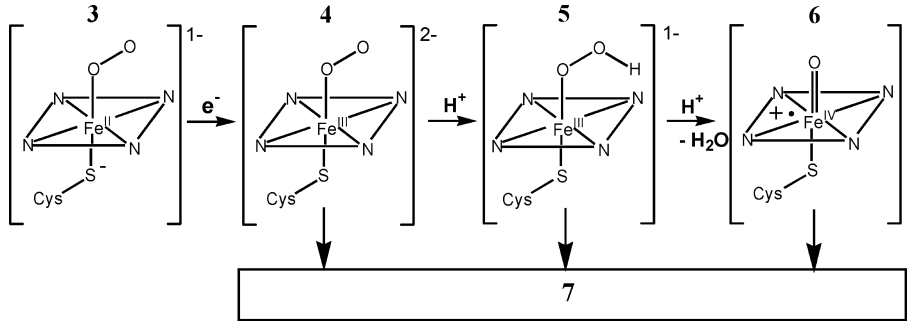

of the reactive intermediates that form during reaction of native P450s,[13] heme oxygenase,[23] and oxy endothelial (e) NOS_{ox}.[24] Cryoreduced oxy-heme species trapped at 77 K largely retain the conformations of the oxy-ferrous heme precursors, and then study by EPR/ENDOR spectroscopies reveals structural features of the heme centers relevant to the parent diamagnetic oxy complexes. Subsequent step annealing controls the reactivity of the reduced enzyme states. This allows for the accumulation of enzymatic intermediates and product states for EPR/ENDOR analysis. In addition, the kinetics of these conversions can be characterized, as well as the associated effects of isotopic substitution.[25] Altogether, these measurements can determine the active intermediates in the enzymatic cycle and reveal key details of the catalytic process.

Radiolytic reduction at 77 K of oxy-$eNOS_{ox}$ both with bound Arg or NOHA and in the presence of 4-aminotetrahydropterin (an inactive BH4 analogue) yields the peroxy-ferri NOS intermediate **4**.[24] Intermediate **4** converts Arg to a product with EPR spectra characteristic of NOHA coordinated to heme at the relatively low temperature of 165−170 K. EPR and proton ENDOR spectra of the primary product state with Arg as substrate (**7**) support the suggestion that the reaction involves the formation and attack of **6** on the Arg guanidinium group. However, at no stage of the reaction/annealing process does one observe an EPR signal from **5** with either substrate. This is in sharp contrast to the other heme enzymes, such as the cytochromes P450[13,26] and heme oxygenase.[23] Extending these studies with eNOS was difficult because oxy-eNOS complexes are unstable at high protein concentrations.

Recently it was reported that gsNOS forms an especially stable oxy complex **3**,[11] unlike the mammalian NOSs. Like mammalian NOSs, the Soret band of oxy Fe(II)gsNOS red-shifts in the presence of substrates,[11] and the shift correlates with hydrogen-bonding/or electrostatic interactions between the guanidine group of substrates and the heme-bound dioxygen.[11,27] This stability of **3** makes gsNOS a particularly favorable subject for cryoreduction EPR/ENDOR studies of the mechanisms of both Stage I hydroxylation of L-Arg to form NOHA and Stage II oxidation of NOHA to citrulline and NO. In this report we describe such experiments and show that they provide strong evidence for Cpd I (**6**) as the reactive species in Stage I but the hydroperoxo-ferriheme (**5**) as the reactive species in Stage II. These experiments further illuminate the proton-transfer processes that accompany these reactions.

Materials and Methods

Materials. Tris, sodium chloride, ethylene glycol (EG), and ammonium acetate were obtained from Mallinckrodt; urea was obtained from Ambion; sodium tetraborate, 2-mercaptoethanol, *o*-phthalaldehyde (OPA), L-arginine, citrulline (Cit), ethylene glycol-d_2, *N*-methyl-L-arginine, and *N*-nitro-L-arginine were from Sigma; NOHA and methanol were from Fisher Scientific; nitric oxide donor NOC-7 was from Alexis Biochemicals; and D_2O was from Cambridge Isotope Laboratories Inc.

Sample Preparation for Cryoreduction. gsNOS was expressed, purified, and concentrated as described.[11] The concentrated protein was diluted 10 times into 100 mM Tris pH 8.5, 150 mM NaCl, 50% EG (final concentration), and concentrated back to 1 mM. When needed, the protein was exchanged into buffers made using D_2O and EG-d_2. In D_2O buffers, the pH was adjusted to 8.1 (as measured using a pH electrode), which is equivalent to a pH of 8.5 in H_2O buffers.[28] Also, when needed, Arg and NOHA were added in equimolar amounts and Me-Arg, NO_2-Arg, and Cit were added in 5-fold excess to ensure full complex formation. All the Fe(II)-gsNOS samples were made by first incubating the ferric protein in an anaerobic glovebox overnight to remove oxygen from the protein solution and then reducing Fe(III)-gsNOS stoichiometrically using equivalent amounts of dithionite (determined by titration) inside an anaerobic glovebox. An extinction coefficient of 8000 M^{-1} cm^{-1} at 315 nm[29] was used to determine the concentration of dithionite, and an extinction coefficient of 78 800 M^{-1} cm^{-1} at 409 nm was used for gsNOS. Complete reduction of gsNOS without a significant excess of dithionite was confirmed from the absorption spectrum of the reduced gsNOS samples. The samples were then transferred into either EPR or ENDOR tubes as necessary and frozen in liquid nitrogen. NO complexes of gsNOS were prepared by incubating a 3 M excess of NOC-7 with gsNOS for 5 min ($t_{1/2}$ of NO formation from NOC-7 is 5 min at room temperature, pH 7.0, and increases with pH) at room temperature in an anaerobic glovebox, in the presence of a 5 mM excess of dithionite. Oxy-gsNOS complexes were made by first warming the reduced protein in frozen EPR tubes to −30 °C and then bubbling with cold oxygen gas. The samples were then stored in quartz EPR tubes at 77 K until cryoreduction. The majority of cryoreduction experiments with oxy-gsNOS complexes were carried out at pH 8.5 because the oxy-ferrous state exhibits enhanced stability at this pH value.

γ-irradiation of the frozen hemoprotein solutions at 77 K typically was performed for ∼20 h (dose rate of 0.15 Mrad/h, total dose 2−3 Mrad using a Gammacell 220 ^{60}Co.[13] Annealing at temper-

(23) Davydov, R.; Kofman, V.; Fujii, H.; Yoshida, T.; Ikeda-Saito, M.; Hoffman, B. *J. Am. Chem. Soc.* **2002**, *124*, 1798–1808.
(24) Davydov, R.; Ledbetter-Rogers, A.; Martasek, P.; Larukhin, M.; Sono, M.; Dawson, J. H.; Masters, B. S. S.; Hoffman, B. M. *Biochemistry* **2002**, *41*, 10375–10381.
(25) Davydov, R.; Matsui, T.; Fujii, H.; Ikeda-Saito, M.; Hoffman, B. M. *J. Am. Chem. Soc.* **2003**, *125*, 16208–16209.
(26) Davydov, R.; Razeghifard, R.; Im, S.-C.; Waskell, L.; Hoffman, B. M. *Biochemistry* **2008**, *47*, 9661–9666.
(27) Marchal, S.; Gorren, A. C. F.; Sorlie, M.; Andersson, K. K.; Mayer, B.; Lange, R. *J. Biol. Chem.* **2004**, *279*, 19824–19831.
(28) Glasoe, P. K.; Long, F. A. *J. Phys. Chem.* **1960**, *64*, 188–190.
(29) Dixon, M. *Biochim. Biophys. Acta, Bioenerg.* **1971**, *226*, 241–258.

atures over the range 77−270 K was performed by placing the EPR sample in the appropriate bath (e.g., *n*-pentane or methanol cooled with liquid nitrogen) and then refreezing in liquid nitrogen.[13,23,24]

Analysis of Reaction Products after Cryoreduction and Annealing. For product identification, 6 M urea (final) was added to the protein solution to dislodge products from enzyme. To remove protein from solution, the samples were centrifuged through a filtering unit (10 kDa MW cutoff), and the flow-through, which contains the amino acids, was collected. The amino acids were then derivatized using OPA as described,[30] and the ensuing products were analyzed using reverse-phase HPLC. The samples were run through an HP ODS Hypersil 5-μm 100 × 21 mm C18 column and detected by fluorescence (excitation, 360 nm; fluorescence, 465 nm). The elution method described in ref 30 was modified as follows: The column was equilibrated with 5 mM ammonium acetate (pH 6.0), 20% methanol (v/v) (solvent A) run at 1 mL/min at room temperature. The elution conditions for the amino acid-OPA derivatives were 100% solvent A for 2 min, 0−50% solvent B (methanol) over 39 min, a linear increase to 100% solvent B over 3 min and continue at 100% solvent B for 5 min, and a return to 100% solvent A over 3 min and continue with 100% solvent A for 3 min. Elution times for Arg (22.6 min), NOHA (20.5 min), and Cit (16.1 min) were determined using standards and were compared to those of the products of the cryoreduction and annealing reactions. Tris, also a primary amine at pH 10 (like the amino acids), was present in the buffers and reacted with OPA to give a fluorescent product (elution time, 19.4 min). All of the product peaks were well resolved. The elution peak (measured by fluorescence) for the NOHA-OPA derivative was smaller than those for Arg and Cit, although they were all present in equimolar amounts, as has been previously described.[30] The absorbance trace (at 360 nm) revealed similar peak heights, confirming that equimolar amounts of amino acids were present. Other small elution peaks that were observed in the reaction mixture after cryoreduction and annealing had much smaller absorbance, indicating that they were minority components compared to the major reactants/products present in the irradiated samples and were not identified.

EPR/ENDOR Spectroscopy. X-band CW EPR spectra were recorded on a Bruker ESP 300 spectrometer equipped with an Oxford Instruments ESR 910 continuous He flow cryostat. CW 35 GHz EPR/ENDOR spectra were recorded on a modified Varian E-109 spectrometer. All CW Q-band EPR/ENDOR spectra were recorded at 2 K in dispersion mode under "rapid passage" conditions, which gives an absorption line shape. The EPR signals of cryogenerated species were quantitated using 0.5 mM low-spin substrate-free ferric P450 2B4 as standard. For a single orientation of a paramagnetic center, the first-order ENDOR spectrum of a nucleus with $S = 1/2$ in a single paramagnetic center consists of a doublet with frequency given by[31]

$$\nu_{\pm} = |\nu_N \pm A/2|$$

Here, ν_N is the nuclear Larmor frequency, and A is the orientation-dependent hyperfine coupling constant of the coupled nucleus. The doublet is centered at Larmor frequency and separated by A when $\nu_N > A/2$, as is the case for the ^{1}H spectra presented here. Hyperfine tensors were determined by analysis of 2D patterns comprised of ENDOR spectra collected across the EPR envelope, as described elsewhere.[31]

As shown previously, γ-irradiation at 77 K yields an intense EPR signal at $g = 2.0$ from radiolytically generated organic radicals; such signals are truncated in the reported spectra for clarity. In addition, γ-irradiation produces hydrogen atoms within the fused silica tubes, and these give a characteristic hyperfine doublet ($A(^1H) \approx 507$ G). As seen in all cases, as the annealing temperature is raised, radical recombination occurs, and both the radical and H-atom signals decrease.

Optical absorbance spectra at 77 K were acquired from samples in EPR tubes in a quartz "finger-dewar" with an Ocean optics USB2000 spectrophotometer.

Table 1. **g**-Tensor Components for Fe(III)-gsNOS Complexes

substrate	species	g_1	g_2	g_3
none	ls (major)	2.42	2.28	1.916
	ls	2.50	2.28	1.88
	hs	7.77	4.01	1.79
Arg	hs (major)	7.78	4.0	1.79
	ls	2.43	2.286	1.912
	ls	2.49	2.28	1.87
NOHA	hs (major)	7.85	3.92	1.77
	ls	2.427	2.28	1.912
	ls	2.51	2.28	1.884
Me-Arg	hs (major)	7.85	3.93	1.77
	ls	2.42	2.28	1.91
NO_2-Arg	hs (major)	7.55	4.27	1.84
	ls	2.43	2.28	1.91(5)
Cit	ls	2.52	2.30	1.87
	ls	2.42	2.29	1.91(4)
	hs	7.75	4.06	1.79(4)
ThioCit	ls	2.71	2.28	1.79
	hs	7.56	4.18	1.83
Im	ls	2.53	2.29	1.86
	ls	2.60	2.29	1.83

Results

Effect of Substrates and Inhibitors on EPR/ENDOR of Ferri-gsNOS Heme Site. We have studied the effect of substrates, products, and inhibitors on the EPR spectra of ferric gsNOS to compare the properties of gsNOS complexes with these of mammalian NOSs. Importantly, the ferriheme spectra provide reference data for use below in assigning specific states to the EPR spectra of oxy-gsNOS complexes that have been subjected to cryoreduction/annealing.

Although at ambient temperature substrate-free (sf) ferric gsNOS at pH 7.4 shows an optical absorption spectrum with a Soret band at 403 nm, characteristic of a high-spin, pentacoordinate ferriheme,[11] the low-temperature EPR spectrum of sf ferric gsNOS in 50% EG/buffer pH 8.5 exhibits a low-spin EPR signal with $\mathbf{g} = [2.42, 2.28, 1.916]$ (Table 1; Supporting Information, Figure S1), characteristic of the hexacoordinate aquoferric form. A similar change in spin state at low temperature is observed for high-spin forms of cytochromes P450. In addition, extended incubation of sf ferric $eNOS_{ox}$ at 4 °C was reported to substantially increase the proportion of a low-spin conformer.[32] The coordinated water of sf aquo-ferri-gsNOS exhibits exchangeable ^{1}H ENDOR signals from the bound water, with maximum hyperfine coupling $A \approx 10$ MHz at g_1 (Supporting Information, Figure S2A).

Addition of Arg, NOHA, or arginine analogues Me-Arg or NO_2-Arg causes the enzyme to adopt the five-coordinate, high-spin substrate-bound form with characteristic rhombic EPR signals whose g-values vary with the bound substrate/analogue

(30) Adak, S.; Wang, Q.; Stuehr, D. J. *J. Biol. Chem.* **2000**, *275*, 17434–17439.
(31) Hoffman, B. M. *Acc. Chem. Res.* **1991**, *24*, 164–170.
(32) Salerno, J. C.; Martasek, P.; Williams, R. F.; Masters, B. S. S. *Biochemistry* **1997**, *36*, 11821–11827.

(Table 1; Figure S1). These results are qualitatively quite similar to those reported for eNOS[32] and nNOS.[33] The addition of L-citrulline to Fe(III)-gsNOS causes the appearance of a new low-spin form with $\mathbf{g} = [2.51, 2.29, 1.87]$ (Table 1), similar to the behavior reported for eNOS and nNOS.[33,34] This state shows an ^{1}H ENDOR signal with $A_{max} \approx 13$ MHz at g_1 that exchanges upon D_2O substitution (Figure S2B). This result indicates that the Cit amide carbonyl does not coordinate to the Fe(III). This hyperfine value is sufficiently close to that for heme-bound water to permit such an assignment, but the structure of Fe(III)-bsNOS/Cit showed that Cit binds to the active site in a conformation very similar to that of L-Arg or NOHA (unpublished data), with the Cit amino group close to the heme iron(III), and such a ^{1}H interaction may instead come from the Cit NH_2 bound to Fe. In support of this possibility, we have found that the ε-NH_2 group of Lys79, coordinated to the heme iron(III) of alkaline cytochrome *c*, gives a similar strongly coupled exchangeable ^{1}H ENDOR signal with $A_{max} \approx 16$ MHz, while in native ferricytochrome *c*, with Met-80 as the sixth axial ligand, this signal is absent. As additional evidence against Cit carbonyl coordination, neither imidazole nor thiocitrulline (Table 1; Figure S1) shows such a strongly coupled exchangeable ^{1}H signal when bound to Fe(III) of gsNOS (Supporting Information, Figure S3).

The strong similarities between the EPR spectra of the ferric forms of mammalian and gsNOS are as expected from the high degree of structural similarities between the heme environments in these proteins.

Cryoreduced Oxy-gsNOS. Figure 2 presents EPR spectra of cryoreduced substrate-free oxy-gsNOS and its complexes with substrates and inhibitors. The spectrum from the substrate-free enzyme shows a majority species whose rhombic EPR signal, $\mathbf{g} = [2.30, 2.21, \text{nd}]$ (Table 2) is characteristic of a hydroperoxy-ferric heme species, **5**,[13,35] showing that the peroxo ligand formed by 77 K cryoreduction of **3**/sf is promptly protonated.

The properties of the resulting **5** are modulated when different substrates and analogues are bound (Figure 2, Table 2). The EPR spectrum of cryoreduced oxy-gsNOS/Arg (**3**/Arg) exhibits two EPR signals, which indicates the presence of two conformational substates in the **3**/Arg precursor. The **g**-tensor of the major signal, $\mathbf{g} = [2.30, 2.16, <1.94]$, again is characteristic of a hydroperoxy-Fe(III) heme intermediate (**5**). Figure 3 shows the 2D field/frequency pattern of ^{1}H ENDOR spectra collected from **5**/Arg at selected **g**-values across its EPR envelope. The spectra exhibit strongly coupled exchangeable proton ENDOR signals, with the maximum hyperfine coupling, $A_{max} = 10$ MHz, characteristic of the hydroperoxo proton.[13] Simulations of the 2D ENDOR pattern gave as a best fit an axial hyperfine tensor dominated by the isotropic component, $a_{iso} = 6.8$ MHz, $2T(^1\text{H}) = 3.2$ MHz, both parameters being typical of **5**. Substrate-free **5** shows similar ^{1}H ENDOR spectra (not shown).

The observation of **5** as the product of 77 K cryoreduction in the substrate-free enzyme and as the majority form for the Arg-bound enzyme indicates that a hydrogen-bonding network to the dioxygen ligand supports proton delivery at 77 K in sf and Arg-bound gsNOS. However, the **g**-values of the sf and Arg-bound enzyme differ slightly (Table 2), which indicates

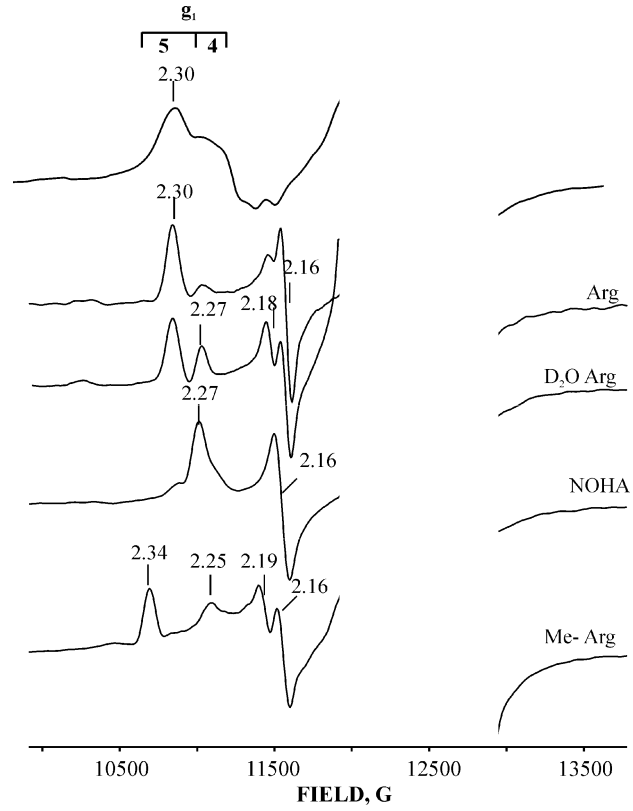

Figure 2. Effect of substrates and inhibitors on 35 GHz EPR spectra of cryoreduced **3**. Braces at top show range of yields expected for g_1 of species **4** and **5**. Conditions: $T = 2$ K, modulation amplitude (Am) = 2 G, microwave frequency = 34.995 GHz.

that the bound substrate perturbs the geometry of the oxy-heme moiety, consistent with reported optical spectroscopic data.[11,27] The minor species in the spectrum of cryoreduced **3**/Arg shows the smaller spread in **g**-values (Table 2) characteristic of a peroxo-ferric intermediate, **4**/Arg. The relative contribution of this minor species increases noticeably in deuterated solvent (Figure 2), the result of solvent KIE in the protonation of the peroxo ligand.

Cryoreduction of oxy-gsNOS-BH4/L-Arg yields a majority **5**-BH4/L-Arg species with an EPR spectrum little different from that of **5**/L-Arg, although the presence of BH4 does cause the appearance a new, rather weak low-spin ferriheme EPR signal, $\mathbf{g} = [2.57, 2.18, \sim 1.87]$ (Supporting Information, Figure S4; Table 2).

The EPR spectrum of cryoreduced **3**/Me-Arg exhibits a majority signal from **5**/Me-Arg, with a minority signal from **4**/Me-Arg, just as with the Arg ternary complex. ^{1}H ENDOR spectra of **5**/Me-Arg show well-resolved signals from the proton of the hydroperoxy ligand to heme Fe(III), with maximum hyperfine coupling of 11 MHz (Figure 4), very much like the signals associated with **5**/Arg. Nonetheless, Arg methylation causes distinct changes to the **g**-values of the peroxo and hydroperoxo species (Table 2). These differences may reflect either a direct interaction of the substrate methyl group with bound dioxygen or its perturbing effects on the protein environment of the oxy-heme site. In contrast, NO_2-Arg curiously has little effect on the EPR spectrum of the cryoreduced oxy-heme center (Supporting Information, Figure S5; Table 2).

Unlike *any* of the oxy-gsNOS complexes considered above, 77 K reduction of **3**/NOHA produces a species with the narrower **g**-spread ($g_1 = 2.27$), characteristic of a peroxo-ferric species,[13,35]

(33) Kominami, S.; Yamazaki, T.; Koga, T.; Hori, H. *J. Biochem. (Tokyo)* **1999**, *126*, 756–761.
(34) Salerno, J. C.; McMillan, K.; Masters, B. S. S. *Biochemistry* **1996**, *35*, 11839–11845.
(35) Davydov, R.; Chemerisov, S.; Werst, D. E.; Rajh, T.; Matsui, T.; Ikeda-Saito, M.; Hoffman, B. M. *J. Am. Chem. Soc.* **2004**, *126*, 15960–15961.

Table 2. **g**-Tensor Components for 77 K Cryoreduced Oxy-gsNOS Complexes and the Intermediates Arising during Their Annealing

substrate	species	T_{an} (K)		g_1	g_2	g_3
		gsNOS				
−	**5**/sf	primary		2.30	2.21	nd
Arg	**5**/Arg	primary	major	2.31	2.16	nd
	4/Arg	primary	minor	2.27	2.18	nd
	g-2.5	145	major	2.50	2.25	1.88
	g-2.48		minor	2.48	2.25	1.91
	g-2.5	175		2.50	2.25	1.88
Arg + BH4	**5**/Arg	primary	major	2.30	2.16	nd
			minor	2.57	2.18	∼1.87
	4/Arg	primary	minor	2.27	2.18	nd
	g-2.47	145	major	2.46	2.24	1.91
	g-2.5		minor	2.50	2.25	1.88
	g-2.5	195		2.50	2.25	1.88
NOHA	**4**/NOHA	primary		2.27	2.16	nd
	5/NOHA	160		2.36	2.22	1.93
	g-2.47	170	major	2.47	2.26	1.91
	g-2.49		minor	2.49	2.26	1.91
Me-Arg	**5**/Me-Arg	primary	major	2.34	2.16	nd
	4/Me-Arg	primary	minor	2.25	2.19	nd
	g-2.26	145		2.26	2.19	1.96
	g-2.5	185		2.48	2.26	1.91
				2.55	2.26	1.89
				2.58	2.26	1.86
NO_2-Arg	**5**/NO_2−Arg	primary		2.30	2.20	nd
	4/NO_2−Arg	primary		2.27	2.16	nd
		eNOS[24]				
Arg	**4**/Arg	primary		2.26	2.16	
	g-2.59	166		2.59	2.25	1.84
	g-2.54			2.54	2.25	1.86
	g-2.59	205		2.59	2.25	1.84
NOHA	**4**/NOHA	primary		2.26	2.15	∼1.95
	g-2.48	166		2.48	2.23	nd
	g-2.44			2.44	2.29	1.90

4/NOHA, and with *g*-values (Table 2) very close to these reported for **4**/NOHA formed in eNOS.[24] This implies that perturbations in the hydrogen-bonding network by bound NOHA impedes the 77 K delivery of a proton to the basic peroxy ligand of the gsNOS ferriheme, just as in eNOS.

An orientation-selective, 2D field/frequency ENDOR pattern for **4**/NOHA discloses an exchangeable ^{1}H ENDOR signal with maximum hyperfine coupling, $A_{max} \approx 9.5$ MHz (Figure 5). This can be attributed to an H-bond to the peroxy ligand, analogous to the H-bonds seen in the cryogenerated **4** of other heme proteins, possibly from the NOHA hydroxyl or the protonated N^{ω} NOHA nitrogen, which is directed toward the heme Fe. The magnitude of A_{max} for **4**/NOHA is similar to those for the cryogenerated peroxy-ferric myoglobin and adult hemoglobin α-chains, although less than the 15−19 MHz observed, for example, for the cryogenerated peroxo-ferric hemoglobin *β*-chains.[36] The differences likely reflect differences in H-bond geometry, perhaps with one class having the H-bond directed to the O remote from Fe and the other having the H-bond to the proximal O. DFT computations could address this issue profitably.

Absorption Spectra. Optical spectra of the ternary complexes of oxy-NOS also can help to establish the protonation state of bound substrates and analogues. Binding of NOHA or Arg to oxy-NOSs causes a significant red-shift of the Soret band, and this was explained in terms of a shift of electrons/charge from

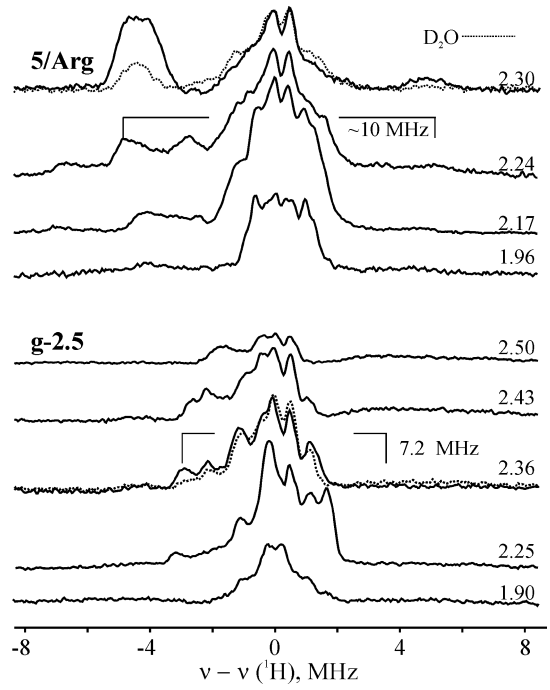

Figure 3. ^{1}H 35-GHz CW ENDOR spectra of cryogenerated **5**/Arg with ^1H_2O buffer and after annealing at 175 K for 1 min (**g-2.5** species), taken at indicated **g**-values. (Weaker signals with $A_{max} \approx 15$ MHz come from **4**/Arg.) Spectra with deuterated solvent shown by dotted line. Conditions: $T = 2$ K, Am = 1 G, rf sweep rate = 0.5 MHz/s, 15 scans.

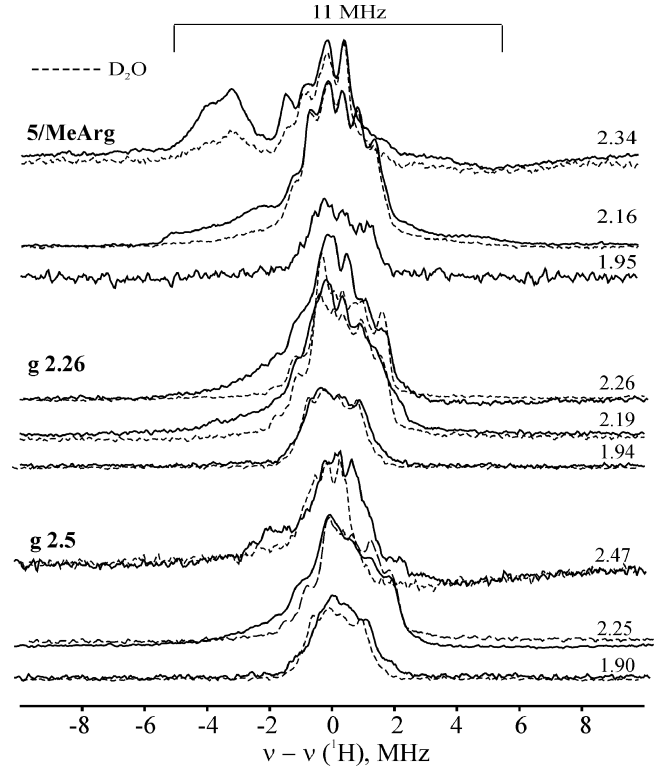

Figure 4. ^{1}H 35 GHz CW ENDOR spectra of **5**/Me-Arg, after annealing at 156 K for 3 min (**g-2.26** species), and after annealing at 170 K for 1 min (**g-2.5** species). Conditions: $T = 2$ K, Am = 1 G, rf sweep rate = 0.5 MHz/s, bandwidth broadening = 50 kHz, 20 scans.

(36) Davydov, R.; Behrouzian, B.; Smoukov, S.; Stubbe, J.; Hoffman, B. M.; Shanklin, J. *Biochemistry* **2005**, *44*, 1309–1315.

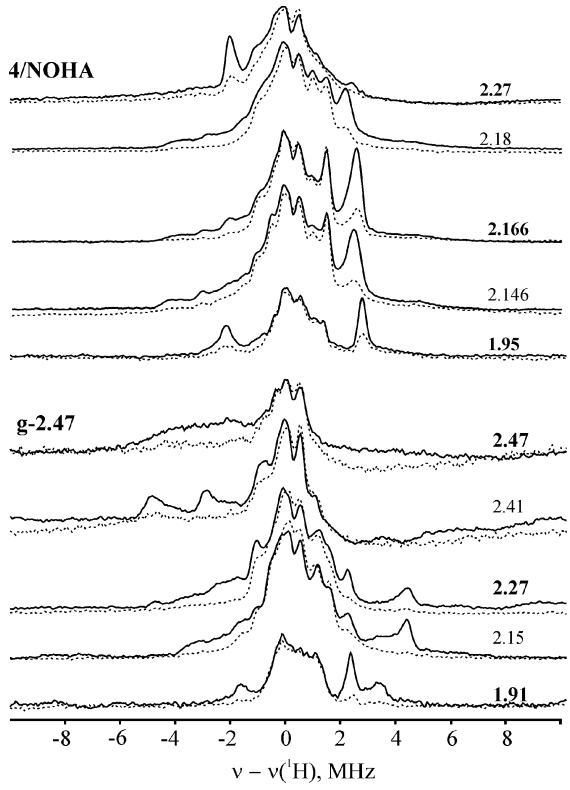

Figure 5. ^{1}H 35 GHz CW ENDOR spectra of cryogenerated **4**/NOHA in H_2O (solid line) and D_2O (dotted line) buffers, and for the **g-2.47** species formed by annealing at 160 K for 350 min. Conditions as in Figure 3.

the heme Fe(II) toward bound O_2[11,27] that is induced by the positively charged substrate. Likewise, we find that the Soret band of oxy-gsNOS at 77 K is shifted from 415 to 426−428 nm in the presence of Arg, NOHA, and Me-Arg, respectively (not shown), suggesting that all three residues are probably charged.

The cryoreduced ternary oxy-gsNOS complexes with Arg and NOHA show absorption spectra with Soret, β-, and α-bands at 444, 537, and 573 nm and at 441, 535, and 566 nm, respectively (Supporting Information, Figure S6), characteristic of thiolate-coordinated, one-electron-reduced oxy-heme moieties.[37]

NO-Fe(II)gsNOS. The perturbing effects of bound substrate on the oxy-heme moiety of gsNOS also are visible in EPR spectra of complexes of Fe(II)NOS with the dioxygen analogue, NO. Figure S7 in the Supporting Information exhibits the EPR spectra of the NO complexes of NO-Fe(II)gsNOS and of the ternary complexes with Arg, Me-Arg, and NOHA. These spectra strongly resemble those reported for respective NO complexes of mammalian nNOS,[38] with the rhombic cytochrome P450-type EPR spectra typical of a hexacoordinate NO-heme complex with non-nitrogenous proximal axial heme ligand.[38] Binding L-arginine and its analogues alters the **g**-tensor rhombicity as well as the resolution of ^{14}N hyperfine structure for bound NO. More significant changes are seen in the EPR spectrum of ferrous NO complexes in the presence of NOHA (Figure S7). The spectrum is less anisotropic than those of the substrate-free and the L-Arg-bound NO complexes, with distinctly different **g**-values (Figure S7). Notably, the effects of substrate

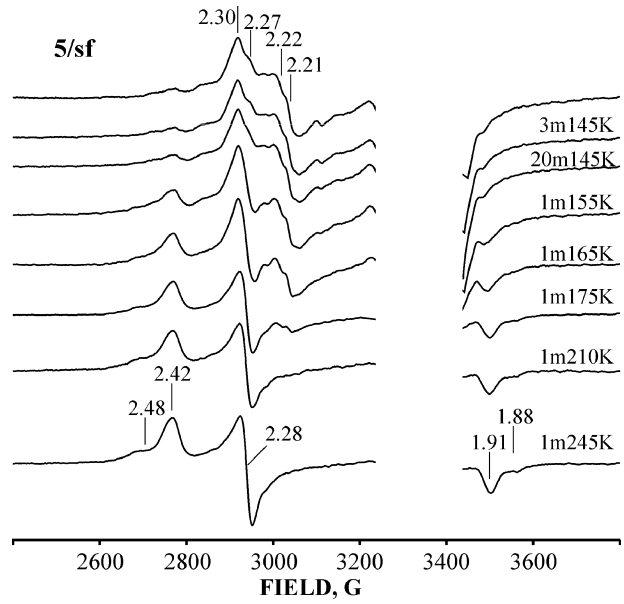

Figure 6. X-band EPR spectra of **5**/sf annealed at the indicated temperatures. Conditions: T = 28 K, Am = 10 G, power = 10 mW, 9.375 GHz.

on the heme site of NO-gsNOS are essentially the same as those reported for mammalian NOS,[38] which again emphasizes the structural similarity between heme sites in gsNOS and mNOSs (Supporting Information).

Annealing of the Cryoreduced Oxy-gsNOS Intermediates. Cryoreduced oxy-gsNOS samples were annealed at progressively higher temperatures, as described previously,[13] and examined by EPR and ENDOR after each step. These experiments enable us to trap and characterize intermediates that occur along the NOS monoxygenase reaction pathway.[13,23,24] Unfortunately, optical spectroscopy is not useful in this endeavor, as these spectra do not distinguish among the intermediates that form during the reaction.

5/sf. The simplest results were obtained upon annealing **5**/sf. Figure 6 presents EPR spectra of this cryogenerated intermediate at progressively higher temperatures. Its signal decreases in intensity during annealing, with the simultaneous appearance of the EPR signal characteristic of low-spin aqua-ferric gsNOS (**g** = [2.42, 2.28, 1.91], Figure 6) and without formation of spectroscopically detectable intermediates. This relaxation of the cryogenerated **5**/sf to the resting state is complete at 175 K. This conversion probably occurs via the very reactive Cpd I, because the pentacoordinate high-spin intermediate would be expected if **5** decays by dissociation of hydrogen peroxide. The same annealing pattern is seen for **5**/NO_2Arg (Figure S5).

5/Arg. Figure 7 shows EPR spectra taken during annealing of cryoreduced **3**/Arg at successively higher temperatures. During this process, the dominant hydroperoxo-ferric species **5**/Arg decays almost completely at the low temperature of 145 K. This decay is accompanied by the parallel appearance of the primary product, **7**, which exhibits two new low-spin signals with similar rhombic **g**-tensors: **g**(dominant) = [2.50, 2.25, 1.88]; **g**(minor) = [2.48, 2.25, 1.91] (denoted as **2.5** and **2.48** species, respectively) (Figure 7, Table 2). Notably, the minority **4**/Arg species disappears completely after annealing at 145 K for 1 min. Further annealing at 175 K results in conversion of the **2.48** species into the **2.5** species (Figure 4). The intensity of the EPR signal of the latter does not change upon annealing

(37) Denisov, I. G.; Makris, T. M.; Sligar, S. G. *J. Biol. Chem.* **2001**, *276*, 11648–11652.
(38) Migita, C. T.; Salerno, J. C.; Masters, B. S. S.; Martásek, P.; Ikeda-Saito, M. *Biochemistry* **1997**, *36*, 10987–10992.

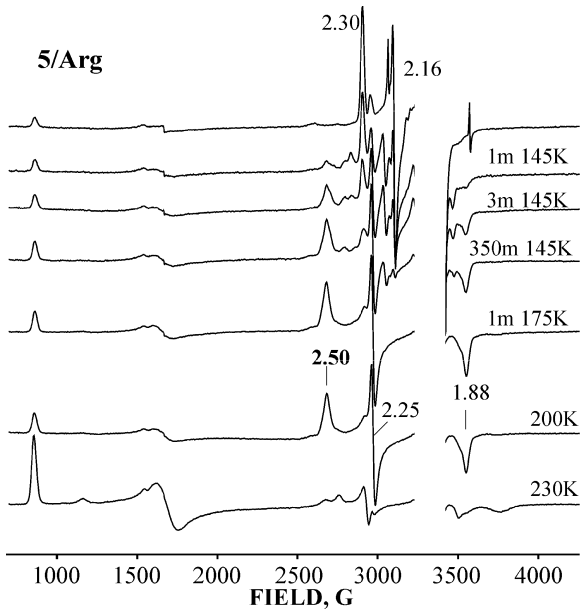

Figure 7. X-band EPR spectra of **5**/Arg annealed under indicated conditions. Conditions: T = 15 K, Am = 10 G, power = 2 mW, 9.365 GHz.

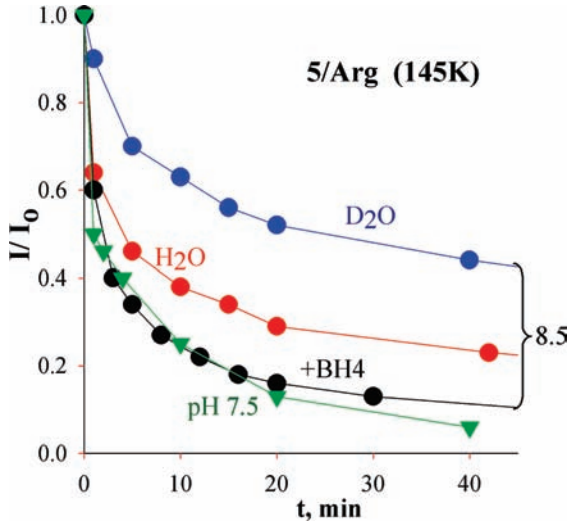

Figure 8. Relative EPR intensity of **5**/Arg ($I/I_0 = I(t)/I(0)$) vs time during step-annealing at 145 K: H_2O buffer, pH 8.5 (red); + BH4, pH 8.5 (black); D_2O buffer, pD 8.5 (blue); pH 7.5 (green); all buffers, 50% EG.

at 200 K for 1 min (Figure 7), but the signal disappears completely at 230 K, and the EPR spectrum of resting ferric state appears (Figure 7, Table 2). HPLC analysis of the irradiated sample, after it was thawed to room temperature, showed that it contained ~0.3 mM NOHA, which is close to the ~0.4 mM hydroperoxo-ferric species cryogenerated at the start of the experiment (with dose 3 Mr) (Supporting Information, Figure S8). Thus, cryogenerated hydroperoxo-ferric-NOS/L-Arg quantitatively converts bound L-Arg into NOHA, and the **g-2.48** and **2.5** species may be assigned as intermediates in this process.

To characterize the reaction of **5**/Arg, we measured the solvent KIE (s-KIE) for its decay at 145 K. As shown in Figure 8, the half-time of this decay increases about 8-fold in deuterated solvent. The decays themselves can be described with stretched exponential functions, which is characteristic of reactions in frozen matrices at low temperatures[39] and indicates that they

Scheme 2

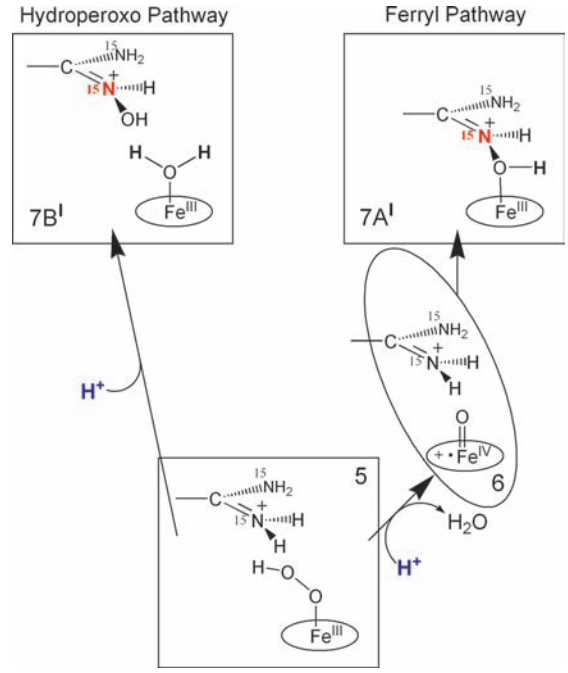

are associated with a distribution of conformational substates. This large s-KIE establishes that under these conditions the rate-limiting step is proton transfer to the hydroperoxy intermediate. Such a reaction could either lead to formation of Cpd I *or* initiate direct reaction of **5** with substrate. The failure to observe the EPR signal from Cpd I during annealing does not eliminate the possibility of its involvement, because Cpd I would not accumulate if it reacted rapidly with protein-bound L-Arg, once formed.

To identify the primary product $\mathbf{7^I}$ (**g-2.48**, **2.5**), and through its nature to infer the reactive heme species of Stage I, we carried out ^{1}H and ^{15}N ENDOR studies on the **g-2.5** major product of Arg hydroxylation. If Cpd I (**6**) were the reactive species, the primary product of Arg hydroxylation would have the hydroxyl group of NOHA bound to Fe(III) ($\mathbf{7A^I}$, Scheme 2). Our early ENDOR measurements on the complex of ferric-nNOS with Arg indicate that if this is the case the **g-2.5** state formed with ^{15}N-Arg should show a ^{1}H ENDOR signal from the bound hydroxyl proton and a ^{15}N ENDOR signal from the oxime N$^{\omega}$.[40] However, if **5** is the reactive species and forms NOHA through direct electrophilic attack on Arg, the ferriheme of the **g-2.5** primary product would have a bound (H_xO), $\mathbf{7B^I}$, and would give ^{1}H ENDOR signals like these observed for low-spin aqua ferric NOS (Figure S2), while the ^{15}N of NOHA would be too remote to give an ENDOR response.

The decisive experiment thus is a ^{15}N ENDOR measurement of the **g-2.5** intermediate prepared with Arg isotopically labeled with ^{15}N at the terminal guanidino nitrogens. Figure 9 compares 35 GHz Mims pulsed ^{15}N spectra for the **g-2.5** species formed during annealing of **5**/L-Arg (^{14,15}N). The spectra of this state with the ^{15}N substrate show a very well-resolved doublet that is centered at the ^{15}N Larmor frequency and that is absent for samples that contain L-Arg (^{14}N). The hyperfine interaction has

(39) Frauenfelder, H.; Young, R. D. *Comments Mol. Cell. Biophys.* **1986**, *3*, 347–372.
(40) Tierney, D. L.; Huang, H.; Martásek, P.; Masters, B. S. S.; Silverman, R. B.; Hoffman, B. M. *Biochemistry* **1999**, *38*, 3704–3710.

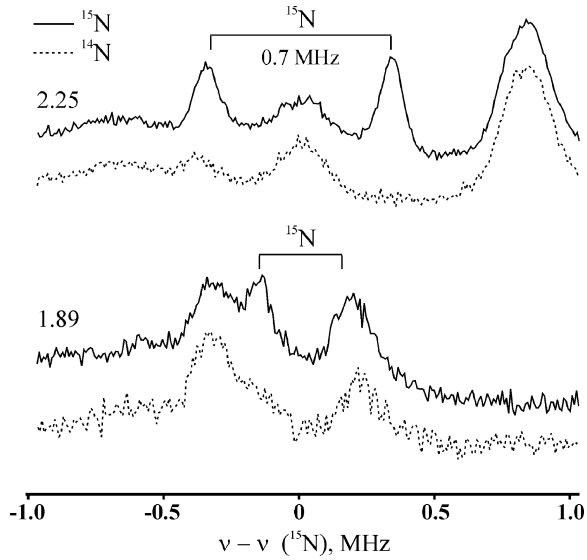

Figure 9. ^{15}N Q-band Mims pulsed ENDOR spectra for the **g-2.5** species formed during annealing of cryoreduced **5**/^{15}N-Arg (solid line) and **5**/^{14}N-Arg (dotted line), taken at indicated **g** values. $T = 2$ K. Pulse conditions: microwave pulse lengths 50 ns, $\tau = 600$ ns, RF pulse length 20 μs, repetition time 20 ms. Number of transients: 700 (**g** = 2.25), 300 (**g** = 1.89).

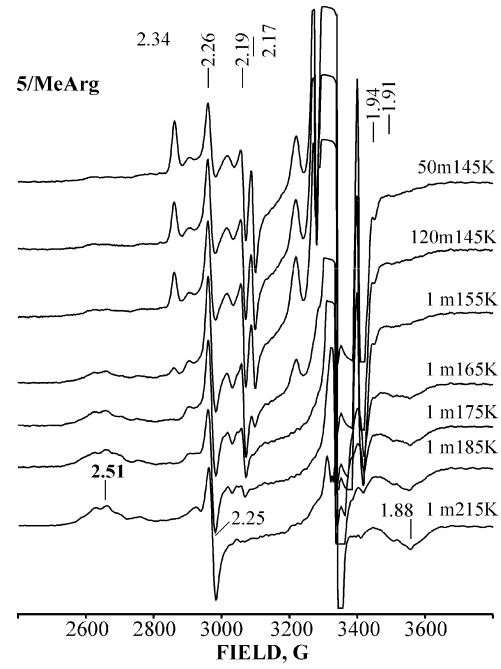

Figure 10. Annealing of the cryogenerated **5**/Me-Arg. Conditions as in Figure 6.

a maximum value at g_1, $A_{max} = 0.7$ MHz. It is dominated by the through-space dipolar interaction and corresponds to an Fe−N distance of r(Fe···N) ≈ 3.5 Å, well within the range expected for NOHA bound to the ferriheme iron by its hydroxyl. Assignment of the **g-2.5** form of the primary product to such a structure **7A^{I}** indicates that L-Arg has been hydroxylated by Cpd I (Scheme 2). In support of this interpretation, we note that the precursor **5**/L-Arg [^{15}N] state exhibits no detectable ^{15}N ENDOR signal because of the longer distance between Fe(III) and the guanidine ^{15}N of L-Arg, which are separated from each other by the hydroperoxide ligand, much as ^{15}N of NOHA would be separated from Fe(III) by its hydroxyl and product water if the hydroperoxo pathway of Scheme 2 were operative.

Proton ENDOR was used to further characterize the **g-2.5** heme site. Figure 3 shows that the 2D field/frequency patterns of ^{1}H ENDOR spectra collected from the **g-2.5** species at selected **g**-values across its EPR envelope are quite distinct from those of **5**/Arg. The **g-2.5** intermediate has exchangeable ^{1}H ENDOR signals whose maximum hyperfine coupling, $A_{max} =$ 7.5 MHz, is significantly less than that for **5**/Arg and less that $A_{max} \approx 10-12$ MHz characteristic of protons of water or hydroxide ligands coordinated to low-spin Fe(III) heme (Figure S2). It is closer to $A_{max} = 9.2$ MHz reported for the hydroxyl proton of 5-hydroxycamphor coordinated to ferric P450cam.[13] These observations are compatible with assignment to the proton of a bound NOHA hydroxyl, which has a weaker bond to heme iron(III) compared to that of H_xO.[41]

We investigated the effects of BH4 on the reaction of **5**/Arg. The **5**-BH4/L-Arg complex also reacts at 145 K, but the reaction is several-fold faster than that in the absence of BH4 (Figure 8; Figure S4). This process generates two well-resolved primary product **7** low-spin ferriheme EPR signals, **g** = [2.46, 2.246, 1.907] and **g** = [2.50, 2.25, 1.88]; these are denoted as **g-2.46** and **g-2.50** (Figure S4, Table 2). Early in the annealing of **5**-BH4/L-Arg, the **g-2.46** is dominant, and unlike the behavior without BH4, it converts completely to the **g-2.5** intermediate upon annealing at 195 K (Figure S4).[42] Further stepwise annealing to 230 K causes the loss of the **g-2.5** species and formation of the resting ferric state (not shown). The spectra of the **g-2.46** and **g-2.5** species are very similar to those of the **g-2.48** and **g-2.5** species formed during relaxation of the BH4-free hydroperoxy-Fe(III)NOS-L-Arg intermediate, and they likewise are attributed to two conformational substates of the primary product state **7** in which NOHA is bound to Fe(III).[24]

5/Me-Arg, NO_2-Arg. The annealing pattern for the cryoreduced **3**/NO_2-Arg complex very much resembles that for the cryoreduced **3**/sf (Figure S5). In both, the state **5** is produced by cryoreduction at 77 K and converts directly to the low-spin aquo ferric state upon annealing to 175−240 K; no other EPR-detectable intermediates accompany the process (Figure S5). This observation indicates that NO_2-L-Arg does not react during annealing of cryogenerated **5.**

In contrast to **5**/NO_2Arg, the $g_1 = 2.34$ EPR signal of cryogenerated **5**/Me-Arg decays at 145 K (Figure 10) and a new low-spin ferric species appears, **g** = [2.26, 2.19, ∼1.94] (Figure S4; Table 2). Further step-annealing to 185 K causes the loss of this **g_1-2.26** species and the appearance of several new EPR signals with $g_1 \approx 2.5$ that are reminiscent of the ***g_1*-2.5** NOS primary product species **7** formed during annealing of the **5**/Arg intermediate (Figure 10, Table 2). These $g_1 \approx$ **2.5** signals from the Me-Arg complex convert to resting ferric state upon annealing at 225 K (not shown). In HPLC traces of the annealed sample, the Me-Arg peak is accompanied by a new peak which can be assigned to the product, *N*-hydroxy-*N*-Me-Arg (not shown). Thus, the decay of **5** leads to hydroxylation of *N*-Me-Arg.

The immediate product of the decay of **5**/Me-Arg is the **g-2.26** center, whose **g**-tensor surprisingly resembles that of a peroxo-

(41) Lefevre-Groboillot, D.; Frapart, Y.; Desbois, A.; Zimmermann, J.-L.; Boucher, J.-L.; Gorren, A. C. F.; Mayer, B.; Stuehr, D. J.; Mansuy, D. *Biochemistry* **2003**, *42*, 3858–3867.

(42) Davydov, R.; Perera, R.; Jin, S.; Yang, T.-C.; Bryson, T. A.; Sono, M.; Dawson, J. H.; Hoffman, B. M. *J. Am. Chem. Soc.* **2005**, *127*, 1403–1413.

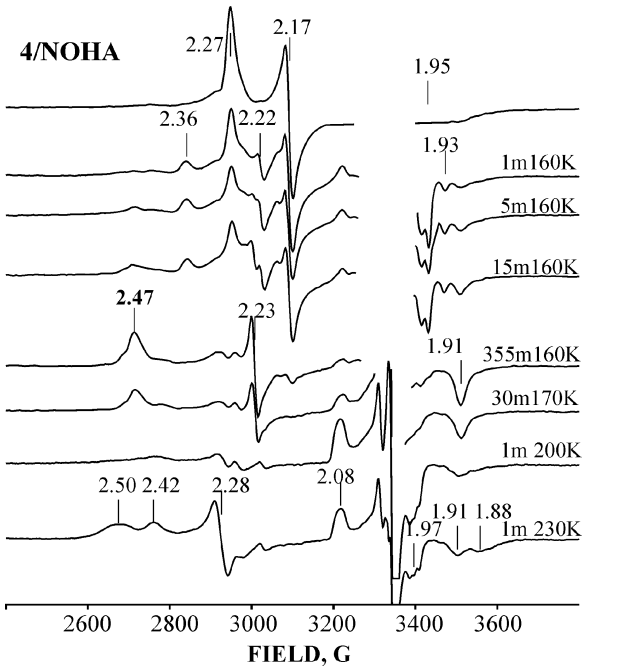

Figure 11. Annealing of cryogenerated **4**/NOHA. Conditions as in Figure 6.

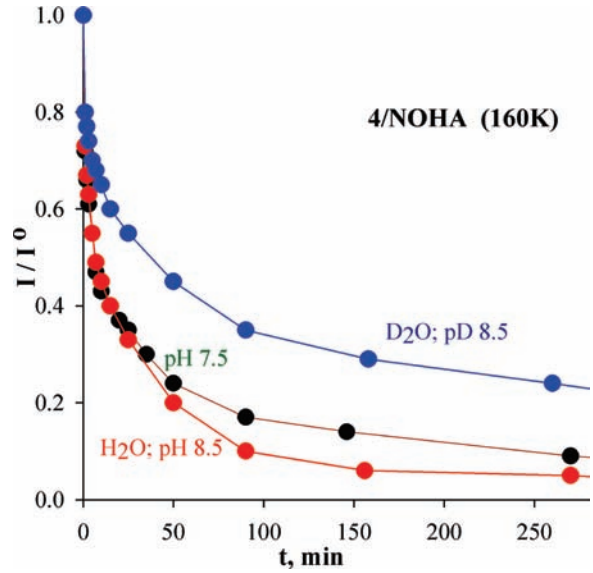

Figure 12. Relative EPR intensity of **4**/NOHA (I/I_0) vs time during step-annealing at 160 K: pH 8.5 H_2O buffer, D_2O buffer; H_2O, pH 7.5 (black); all buffers, 50% EG.

ferriheme species, not a **g-2.5** product species. However, it is unlikely that a hydroperoxo-ferric intermediate would convert back to a peroxo species, which then reacts with Me-Arg, as this requires the presence of a very strong base near the active site and a reversal of the protonation that generated the hydroperoxo upon cryoreduction. A more plausible explanation is that this species is a ferri-NOS product complex having an unusual, nonequilibrium conformation. At higher temperatures, ~165 K, this complex relaxes to a product conformational state showing a $\mathbf{g_1}$**-2.5** signal. In support of this interpretation, Mansuy and co-workers reported that some *N*-hydroxy-guanidines form low-spin complexes with ferric NOS which display rhombic EPR signal with $\mathbf{g} = [2.35-2.38, 2.25, 1.93]$.[41]

These ideas are supported by s-KIE and ^{1}H ENDOR studies. The decay of the cryogenerated **5**/Me-Arg to form the **g-2.26** center is sharply slower in D_2O buffer, with an s-KIE ≈ 6 (Supporting Information, Figure S9), comparable to that for Arg-bound NOS (Figure 8). In contrast, the s-KIE for conversion of the **g-2.26** species to the **g-2.5** intermediate at 165 K is less than 2. Furthermore, the **g-2.26** species and particularly the **g-2.5** species show exchangeable ^{1}H ENDOR signals with $A_{max} < 8$ MHz. (Figure 4), similar to those for the low-spin complex of NOS with NOHA formed during relaxation of cryoreduced **3**/Arg. These observations support the idea that the **g-2.26** species is the product state formed by hydroxylation of bound Me-Arg.

4/NOHA. Progressive annealing of **4**/NOHA at 160 K causes its EPR signal to decay. Early in this process the signal of **5**/NOHA appears, with $\mathbf{g} = [2.36, 2.21, 1.93]$ (Figure 11; Table 2). This in turn decays upon further annealing (Figure 11; Supporting Information, Figure S10), with concomitant appearance of an EPR signal from the primary product, denoted the **g-2.47** state. This low-spin Fe(III) state is formed in two similar conformations, with **g**-tensors, $\mathbf{g} = [2.47, 2.26, 1.91]$ and $\mathbf{g} = [2.49, 2.26, 1.91]$. The intensity of the **g-2.47** product signal continues to increase until decay of **4**/NOHA is complete (Figure 11; Supporting Information, Figure S11). Thus, although **4**/NOHA is trapped during 77 K reduction, **4**/NOHA protonates during reaction at 160 K to form **5**/NOHA, which reacts further to ultimately form the product state **7**. These observations indicate that, during annealing, **4**/NOHA acquires a proton to form **5**/NOHA, which in turn converts to the **g-2.47** primary product. Kinetic measurements for the decay the **4**/NOHA intermediate at 160 K in H_2O/D_2O solvents (Figure 12) show that this decay exhibits s-KIE $\approx 4-5$, consistent with protonation of the peroxy-heme moiety as the rate-limiting step in the decay of **4**/NOHA. The fact that a change of pH from 8.5 to 7.5 has little effect on the kinetics indicates that the immediate proton source is well insulated from bulk solvent—good support for the idea that the proton comes from NOHA (Figure 12).

The **g-2.47** primary product signal shows a well-resolved, strongly coupled ^{1}H ENDOR signal with $A_{max} \approx 10$ MHz (Figure 5), comparable with that for low-spin aqua ferric NOS (Figure S2). From this we conclude that this state contains an aquo-ferriheme. The values of the hyperfine couplings for these **g-2.47** protons likely reflect the perturbing effect of the substrate-derived moiety residing in the heme pocket.

The $\mathbf{g_1}$**-2.47** signal disappears at temperatures above 170 K, and its decay is accompanied by the appearance of an NO-ferroheme EPR signal, $g = 2.079-1.969$ (Figure 11), very similar to that of the substrate-free Fe(II)NOS-NO complex (see Figure S7). The rate constants for the decay of the **g-2.47** species and for the formation of NO-gsNOS are the same (Supporting Information, Figure S12), showing that the **g-2.47** species is a kinetically competent precursor to the NO-Fe(II)-gsNOS state. HPLC analysis of the cryoreduced oxy-NOS/NOHA sample annealed at 273 K shows quantitative conversion of bound NOHA into citrulline (Figure S8).

These results imply that annealing **4**/NOHA at 160 K converts it to **5**/NOHA, which then reacts to form Fe(III)/Cit + HNO/NO^- as the **g-2.47** primary product state, and that during subsequent annealing at 180 K the HNO reacts with the ferriheme to generate the NO-ferroheme (**8**, Scheme 3). Figure S12 in the Supporting Information shows that the reaction of **g-2.47** occurs without a solvent kinetic isotope effect, s-KIE = 1, indicating that loss of proton from HNO does not limit the rate at which the NO-ferroheme state forms.

Scheme 3

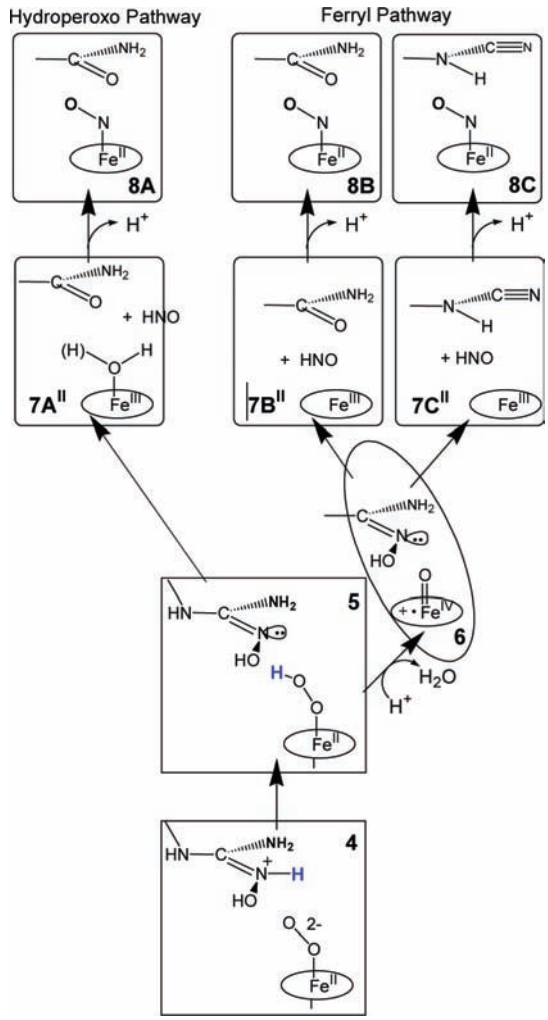

As in the hydroxylation of Arg to form NOHA, the reactive heme species in the conversion of NOHA to Cit + HNO can be inferred from the nature of the primary product, in this case the **g-2.47** state. As depicted in Scheme 3, when Cit is a product of the reaction with NOHA, the primary product is expected to contain the observed aquo-ferriheme when the hydroperoxo-ferric species (**5**) reacts directly with NOHA to form product (**7A^{II}**), whereas this would not be the case if **6** were the reactive state, in which case the product would be a pentacoordinate heme iron and Cit or cyanoornithine (**7B^{II}**, **7C^{II}**). The demonstration by chemical analysis that Cit is formed, plus the ENDOR determination that the **g-2.47** state contains an aquo-ferriheme, thus establishes that the primary product is **7A**, thereby confirming the proposal of Marletta and co-workers that **5**/NOHA is the reactive state in the formation of citrulline/HNO (Scheme 3).[17]

We also investigated the effects of BH4 on the reaction of **4**/NOHA. Although bound BH4 has no noticeable effect on the EPR spectrum of **4**/NOHA, BH4 slows decay of **4**/NOHA and increases the lag period in the appearance of the $\mathbf{g_1}$**-2.47** species (Figure S11). In addition, during 160 K annealing, the appearance of the $\mathbf{g_1}$**-2.47** species is accompanied by that of a low-spin signal with **g** = [2.42, 2.28, 1.91] that can be attributed to aqua ferric-NOS (Supporting Information, Figure S13; Table 2).

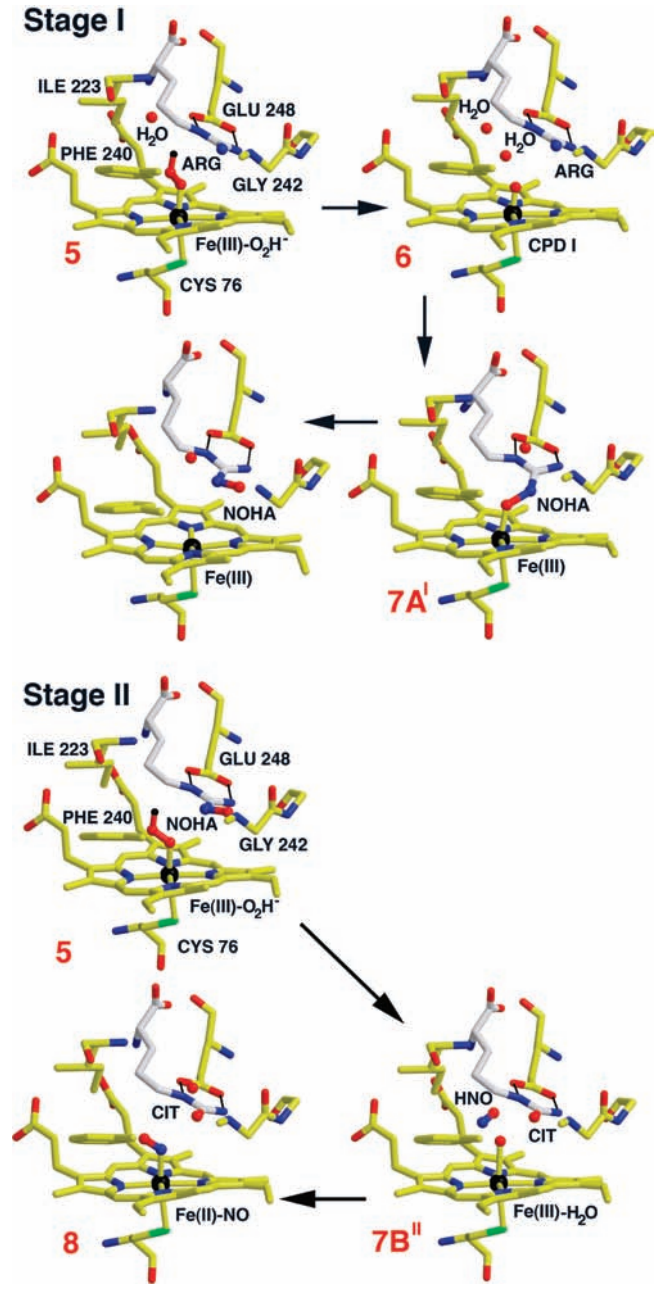

Figure 13. Catalytically active states and primary products of reaction for Stages I and II of the NOS catalytic cycle as revealed by cryo-annealing EPR/ENDOR studies. These representations are based on crystallographic structures of bacterial NOS active centers with substrates and heme ligands bound (PDB codes 1M7V, 1M7Z, 2FC1, 2FBZ) but are purely figurative and not meant to capture the yet uncharacterized conformational changes that likely accompany these states.

Discussion

We have employed cryoreduction and controlled annealing to obtain detailed information about the catalytic cycle of gsNOS by EPR and ENDOR spectroscopies. Furthermore, we apply EPR/ENDOR studies to probe the influence of substrates and inhibitors on the structure of ferri-gsNOS and NO-ferrous-gsNOS. As illustrated in Figure 13, these experiments identify Cpd I (**6**) as the Stage I heme state that hydroxylates Arg to form NOHA but hydroperoxo-ferri-gsNOS (**5**) as the Stage II

state that oxidizes NOHA to Cit and nitroxyl/HNO. These combined results highlight the role of substrates in modulating the activity of a heme monooxygenase.[42]

This section first describes the **5**/[substrate] and **4**/[substrate] states generated by cryoreduction of oxy-NOS/[substrate] complexes and the insights they provide into the structures of the parent oxy-ferrous precursors. This is followed by a discussion of our mechanistic inferences regarding the identities of the reactive heme states and proton delivery processes of Stages I and II, as drawn from the controlled step-annealing of states **4** and **5**.

Cryoreduced 3 and Its Complexes. Cryoreduction of oxy-NOS complexes at 77 K generates EPR-active states that retain the conformation of the oxy precursor[13,43−46] and thus provide a sensitive EPR/ENDOR probe of the diamagnetic oxy-ferrous precursor. The present EPR results show that the properties of oxy-gsNOS change upon binding a substrate and that these changes vary with the structure of the compound.

Cryoreduction of oxy-gsNOS, as well as of oxy-gsNOS complexes with L-Arg, Me-Arg, and NO_2-Arg, yields a hydroperoxo-ferric-gsNOS species (**5**) as the observed product, although *in situ* reduction of an oxy-heme must first form the peroxo-ferriheme, **4**. Previous cryoreduction studies with a variety of oxy-hemoproteins, including P450[13] and HO,[23] showed that such protonation of the basic peroxo ligand of **4**, formed at 77 K or below, requires the presence of an H-bonded proton delivery network in the parent **3** that includes an ordered water molecule in the active site that is hydrogen-bonded to the terminal oxygen of **3**.[13,23,26,44,47,48] This water serves as mediator of proton transfer to the peroxide ligand at 77 K or below.[13,23,35,44,47,48] Perturbation of this network in P450cam by site-specific mutations inhibits this proton delivery and decreases the conversion of cryogenerated **4** to **5**.[13,49] Correspondingly, 77 K cryoreduction of oxyglobins, which do not have such a bound water, exclusively generates **4**, in which a protonated imidazole nitrogen of the distal histidine is H-bonded to the peroxo moiety.[43,45,46] In this case, **4** only becomes protonated at $T > 170$ K, temperatures at which a molecule of water might diffuse into the active site.[50]

Thus, previous measurements on numerous proteins suggest that substrate-free oxy-gsNOS and its complexes with L-Arg, Me-Arg, and NO_2-Arg all contain an active-site water molecule that H-bonds to the terminal oxygen of the dioxygen ligand and participates in the generation of **5** by protonation of **4** formed at 77 K. Moreover, according to Poulos et al., the L-Arg substrate is not in a good position for H-bond donation to the ligand but could donate a hydrogen bond to the water, while the active-site water is capable of hydrogen-bond donation to the O_2.[12,47] We suggest that the protonated guanidinium group of Arg, as well as of some of the analogues, serves as the ultimate proton donor. In support of this, DFT computations suggest that an ordered water itself is a poor proton donor.[51−53]

The structure and behavior of eNOS support this proposal that, in gsNOS, intermediate **5** forms by the delivery of a proton from Arg to **4**/Arg via the bound H_2O. The structure of NO-Fe(II)-eNOS/Arg + BH4 is notably different from those of all other reported crystal structures for CO and NO complexes of mammalian NOSs and bacterial NOS-like proteins in that it does *not* contain an ordered water molecule near the bound diatomic and arginine.[54] Correspondingly, oxy-eNOS/Arg is unlike its gsNOS counterpart in that it yields only the **4**/Arg species as the primary product of 77 K cryoreduction.

The EPR spectra show that binding of L-Arg and its inhibitor analogues modulates the properties of cryogenerated **5** (Table 2). The EPR spectrum of **5**/sf is broad as compared to those of **5**/L-Arg and **5**/Me-Arg (Figure 2). This suggests that O_2 of the parent **3** bound in the absence of substrate can sample multiple conformations and that H-bonding and/or steric interactions in the presence of Arg and analogues stabilize the bound O_2 in a single orientation. This is also evidenced by sharpened ^{14}N hyperfine structure from the bound NO in EPR spectra of **5**/Arg and **5**/Me-Arg (Figure S7). However, cryoreduced **3**/Arg does show a minor peroxo species (Figure 2; Table 2) and hence the presence of a second minority conformational substate. The presence of two substates agrees well with the report of multiple binding conformations of Arg in the heme domain of $mNOS_{ox}$[55] and in the gsNOS-CO complex as well as with structural data reported by Poulos for NO-eNOS.[12,47,54,56−58]

As shown in Table 2, not only does the EPR spectrum of cryogenerated **5**/sf differ significantly from that of **5**/Arg, but the spectra of **5**/Arg and **5**/Me-Arg likewise differ. This indicates different conformations of the hydroperoxy moiety in each of these states, and consequently of the O_2 moiety in the oxy-ferrous parent. The methyl substituent of Me-Arg can alter the positioning of the guanidino substrate relative to the oxy-heme center, as well as altering the interaction of the bound dioxygen with the guanidinium group and an ordered water. Given that during cryoreduction/annealing Me-Arg is hydroxylated at the methylated NH group (see below), as occurs at ambient temperature,[59] the methylated NH rather than the NH_2 group is likely closer to the dioxygen ligand and favorably placed for interactions with the O_2 and with a structural water.

NOHA differs from all other arginine analogues in that 77 K cryoreduction of its complex with oxy-gsNOS yields **4**/NOHA, rather than **5**/NOHA, as observed previously for oxy-eNOS/NOHA.[24] Thus, perturbations in the distal-pocket hydrogen-

(43) Davydov, R.; Kofman, V.; Nocek, J.; Noble, R. W.; Hui, H.; Hoffman, B. M. *Biochemistry* **2004**, *43*, 6330–6338.
(44) Davydov, R.; Satterlee, J. D.; Fujii, H.; Sauer-Masarwa, A.; Busch, D. H.; Hoffman, B. M. *J. Am. Chem. Soc.* **2003**, *125*, 16340–16346.
(45) Unno, M.; Chen, H.; Kusama, S.; Shaik, S.; Ikeda-Saito, M. *J. Am. Chem. Soc.* **2007**, *129*, 13394–13395.
(46) Hersleth, H.-P.; Hsiao, Y.-W.; Ryde, U.; Goerbitz, C. H.; Andersson, K. K. *Biochem. J.* **2008**, *412*, 257–264.
(47) Li, H.; Igarashi, J.; Jamal, J.; Yang, W.; Poulos, T. L. *JBIC, J. Biol. Inorg. Chem.* **2006**, *11*, 753–768.
(48) Schlichting, I.; Berendzen, J.; Chu, K.; Stock, A. M.; Maves, S. A.; Benson, D. E.; Sweet, B. M.; Ringe, D.; Petsko, G. A.; Sligar, S. G. *Science* **2000**, *287*, 1615–1622.
(49) Makris, T. M.; von Koenig, K.; Schlichting, I.; Sligar, S. G. *Biochemistry* **2007**, *46*, 14129–14140.
(50) Kappl, R.; Höhn-Berlage, M.; Hüttermann, J.; Bartlett, N.; Symons, M. C. R. *Biochim. Biophys. Acta* **1985**, *827*, 327–343.
(51) Cho, K.-B.; Derat, E.; Shaik, S. *J. Am. Chem. Soc.* **2007**, *129*, 3182–3188.
(52) Chen, H.; Hirao, H.; Derat, E.; Schlichting, I.; Shaik, S. *J. Phys. Chem. B* **2008**, *112*, 9490–9500.
(53) de Visser, S. P.; Tan, L. S. *J. Am. Chem. Soc.* **2008**, *130*, 12961–12974.
(54) Li, H.; Raman, C. S.; Martásek, P.; Masters, B. S. S.; Poulos, T. L. *Biochemistry* **2001**, *40*, 5399–5406.
(55) Gorren, A. C. F.; Schmidt, K.; Mayer, B. *Biochemistry* **2002**, *41*, 7819–7829.
(56) Rousseau, D. L.; Li, D.; Couture, M.; Yeh, S.-R. *J. Inorg. Biochem.* **2005**, *99*, 306–323.
(57) Li, D.; Kabir, M.; Stuehr, D. J.; Rousseau, D. L.; Yeh, S.-R. *J. Am. Chem. Soc.* **2007**, *129*, 6943–6951.
(58) Kabir, M.; Sudhamsu, J.; Crane, B. R.; Yeh, S.-R.; Rousseau, D. L. *Biochemistry* **2008**, *47*, 12389–12397.
(59) Feldman, P. L.; Griffith, O. W.; Hong, H.; Stuehr, D. J. *J. Med. Chem.* **1993**, *36*, 491–496.

bonding network by bound NOHA impedes the 77 K delivery of a proton to the basic peroxy ligand. Such a chemical effect of bound NOHA on the active site of NOS is paralleled by earlier EPR optical and vibrational spectroscopic observations.[24,38,57,58] These observations suggest that the specific influence of bound NOHA on proton delivery to the one-electron-reduced oxy-heme moiety is characteristic of all NOSs and thus is likely associated with the mechanism of conversion of NOHA into Cit and NO.

Arguments presented above suggest that **4**/NOHA produced by 77 K cryoreduction remains unprotonated because there is no appropriately positioned bound water. Although there are no X-ray structures of oxy-NOS complexes, the structures reported for Arg and NOHA complexes of NO-bsNOS speak to this suggestion.[12] In the NO-bsNOS/NOHA complex, the distance from the nitrogen of NO to the possibly protonated N^{ω} atom of the substrate is short, and water has shifted beyond the distance for a hydrogen bond to the oxygen of NO. In contrast, the L-Arg guanidinium of NO-bsNOS/Arg interacts equally with both atoms of NO, while an active-site H_2O hydrogen-bonds to the distal NO oxygen. Just as the H-bonding to the NO group is different for the two substrates, it is likely that similar differences in H-bonding hinder low-temperature protonation of the peroxo-heme species of **4**/NOHA. In this context the exchangeable proton signal in ^{1}H ENDOR spectra of the cryoreduced oxy-NOS/NOHA complex ($A_{max} \approx 8$ MHz) can be assigned to the NOHA $N^{\omega}H$ H-bonded to the proximal oxygen of heme-bound dioxygen/peroxy ligand.

Taken together these data suggest that 77 K cryoreduction of oxy-gsNOS with bound substrate leads to a majority of **5**/Arg but exclusively to **4**/NOHA because the H-bonding networks surrounding the heme-bound dioxygen are sharply different in the two complexes. In short, the substrate significantly modifies the reactivity of the oxy-heme moiety by modifying this network. The fact that the minor peroxo species **4**/Arg disappears after annealing for a few minutes at 145 K, whereas **4**/NOHA only disappears with a measurable rate after annealing at 160 K, further underscores the differences in the coupling of the H-bonding network to the terminal oxygen of the coordinated peroxo species.

Annealing Measurements. Controlled annealing of **4** and **5** enables a detailed scrutiny of subsequent steps in the catalytic cycle by EPR and ENDOR spectroscopies.[13,23,24] The primary product of reaction, **7**, trapped during progressive annealing has a nonequilibrium structure whose identity, as determined by ENDOR spectroscopy, establishes the nature of the catalytically active heme species. The cryoreduction approach is fully validated by the demonstration that the cryoreduced enzyme is catalytically active and quantitatively hydroxylates Arg to NOHA, as well as NOHA to Cit and HNO.

If the ferryl moiety of Cpd I reacts with the terminal guanidinium nitrogen at low temperature, previous work with cytochromes P450[13] shows that the newly formed hydroxyl group will be coordinated to the ferric heme iron as a nonequilibrium primary product **7** (Scheme 2). In contrast, hydroxylation of substrate by **4**/**5** involves an insertion of the distal peroxy oxygen into substrate, generating the product of this hydroxylation plus forming a stable hexacoordinate ferric form with water/hydroxide as the sixth axial ligand (Scheme 3). This scenario describes heme hydroxylation by cryoreduced oxy-HO.[23] We now show how the step-annealing of **5**/Arg identifies the reactive heme species in Stage I, while that of **4**/NOHA does the same for Stage II (eq 1).

Stage I. The majority **5**/Arg formed by 77 K cryoreduction converts to the low-spin ferriheme **g-2.48** and **g-2.5** intermediates upon annealing at the extremely low temperature of 145 K; further annealing at 175 K results in full conversion into the **g-2.5** species. The decay of **5**/Arg shows a large solvent isotope effect, effective s-KIE ≈ 8, and accelerates at lower pH (Figure 8), which indicates that the rate-limiting step in this process is a proton-assisted reaction of **5**, as expected for conversion into **6**.

The EPR signals of the **g-2.48** and **g-2.50** species (Table 2) resemble those seen previously when the hydroxyl group of a monooxygenation product is coordinated to the heme iron(III).[13,24] In the present study, ^{15}N and ^{1}H ENDOR measurements likewise indicate that state **7** contains NOHA bound to the heme Fe(III) through its hydroxyl OH. As discussed above (Scheme 2), this confirms that hydroxylation of Arg is described by the classic P450 monooxygenase mechanism, with **6** as the active species. The failure to detect **6** by EPR during this process can be accounted for by a high rate of reaction with bound substrate, which prevents accumulation.

The NOHA product present in the **g-2.48/2.5** states is coordinated to the heme iron(III) in a nonequilibrium conformation determined by the initial positioning of Arg in the active site, and it relaxes to the equilibrium form upon further annealing at $T > 145$ K. The presence of two different conformations of the heme-coordinated product in **7** trapped at this earliest stage of product formation reflects the observation that the **5**/Arg precursor state exhibits two conformers; similar behavior was seen for eNOS/Arg (Table 2). Progressive annealing of **7** at temperatures above 200 K results in relaxation of the complex to the equilibrium state in which NOHA remains bound to the protein, but not as a ligand to the ferric heme.

What is the source of the protons for catalysis in the low-temperature process? Evidence presented above suggests that the *first* proton that converts **4** to **5** upon 77 K cryoreduction is delivered from the positively charged guanidinium group of bound Arg via an ordered water initially H-bonded to the O_2 of **3** and thus to the peroxy ligand of cryogenerated **4**. Although there is no crystal structure of **3** for any NOS, this suggestion is supported by the structure of the analogue NO-ferro-NOS (Figure 1), which exhibits such a water.[12,60]

Differences in the source of the *second* proton for catalysis, which is involved in the conversion of **5** to **6**, may account for a notable difference between the Stage I hydroxylation of Arg by gsNOS and reactions of the P450s, both of which have **6** as the reactive species: cryogenerated **5**-gsNOS reacts at the extremely low temperature of 145 K, whereas the P450s react only above 180 K.[13] This is despite the fact that under physiological conditions the monooxygenase activities of P450s are higher than that for gsNOS. In P450s, the second proton for catalysis is likely delivered from beyond the active site,[48] but in NOS this protonation, which is demonstrated by the large s-KIE to be rate limiting in conversion of **5** into **6**, may have as its ultimate donor an ionizable group in close vicinity of the heme coordination site. Possible candidates are the side-chain COOH group of the highly conserved Glu 248, which H-bonds to the guanidinium group, or the heme carboxylates themselves, all of which are predicted to be ~6.5 Å from the site of oxygen binding.[11] Whichever pathway is responsible, it is clearly effective at temperatures of 145 K and above, but not at 77 K.

(60) Li, H.; Poulos, T. L. *J. Inorg. Biochem.* **2005**, *99*, 293–305.

Although the active sites of eNOS and gsNOS are extremely similar, cryoreduction of **3**/Arg at 77 K produces **5**/Arg for gsNOS, whereas its eNOS counterpart exhibits only **4**/Arg and does not accumulate **5**/Arg during conversion to product NOHA at 165 K. This difference likely reflects differences between the hydrogen-bonding networks that provide proton delivery to the oxy-heme moiety in e- and gsNOSs. We suggest that in the **3**-eNOS/Arg complex there is no ordered water adjacent to the peroxy ligand, and that structural relaxation during annealing at 165 K allows a water to approach the peroxy-heme center and convey a proton to **4**. In both enzymes, rapid transfer of the second proton from bound Arg would lead to formation of **6**, which reacts rapidly and does not accumulate. Such behavior is observed during the decay of the cryogenerated **4**-myoglobin. At 180 K and pH 8.2, **4**-Mb quantitatively converts to **5**-Mb, which then slowly converts into Cpd II, whereas at pH < 6.5 **4**-Mb converts to Cpd II without accumulation of EPR-detectable amounts of **5**-Mb because of high rate of its protonation (unpublished data).

Influence of BH4 in Stage I. Addition of BH4 causes a remarkable increase in the rate of conversion of **5**/Arg to the primary products **g-2.46/2.5** and slightly modifies their EPR spectrum. The mere fact that BH4 forms a complex with gsNOS is in line with the data showing that BH4 has a significant effect on the topology of the distal heme binding pocket for mammalian NOSs.[41,61−63] In addition, when BH4 is present, the yield of the **g-2.46** species upon annealing at 145 K increases relative to that for the **g-2.5** species (compare Figures 7 and S4). This indicates that BH4 has a substantial effect on the relative populations of the conformational substates in the precursor **3**/Arg. It further is possible that bound BH4 stabilizes the H-bond network that facilitates proton delivery to the hydroperoxo-heme.[64]

Stage II. When cryogenerated **4**/NOHA is annealed at 160 K, it converts to **5**/NOHA, which in turn reacts to form the **g-2.47** primary product **7**. The large s-KIE for the loss of **4**/NOHA at 160 K (Figure 12) indicates that protonation of the peroxy-heme moiety is the rate-limiting step of this process. The absence of a pH effect on the rate of protonation (Figure 12) indicates that the proton source is local to the oxy complex and sequestered from bulk solvent, which thus supports the proposal that the proton is donated by the positively charged hydroxy-guanidine group of NOHA.[12,60,65]

Chemical analysis shows that the cryoreduction/annealing process quantitatively converts NOHA to Cit, with no detectable amounts of cyanoornithine. EPR shows that the other product of this process is HNO or (NO^-), which reacts with the ferriheme at higher temperature (180 K) to form the EPR-active NO-Fe(II)gsNOS. These two products also form during hydrogen peroxide-supported oxidation of NOHA by mNOS[17,66] and upon use of 4-amino-BH4 as cofactor in the oxidation of NOHA by O_2 as catalyzed by eNOS.[64] HNO is formed by two-electron oxidation of NOHA, whereas formation of NO requires an additional oxidation of nitroxyl, for an overall three-electron oxidation.[67] When BH4 is the reductant of **3**, it is believed the nitroxyl (or its complex with ferric NOS) is oxidized to NO (or the NO complex of Fe(III)NO) by re-reduction of the $BH4^+$ radical formed by the initial reduction.[15]

The ^{1}H ENDOR measurements show that the **g-2.47** ferriheme of primary enzymatic product state **7** in Stage II is coordinated by water rather than by the Cit product, even though Cit is able to form a low-spin complex with the ferriheme; the same is true for oxidation of NOHA during cryoreduction/annealing of oxy-eNOS. As indicated in Scheme 3, when Cit is the product of NOHA oxidation and **7** contains the H_2O-ferriheme, then **5** must be the reactive state. Marletta and co-workers correspondingly concluded that when Cit is the product of NOHA oxidation catalyzed by the iNOS peroxide shunt reaction, then the reactive state is **5**, whereas when cyanoornithine is the product, **6** is the active species.[17,66] Thus, the ENDOR measurements on the **g-2.47** primary product of cryoreduction/annealing are in agreement with the conclusion of Marletta and co-workers regarding ambient-temperature iNOS-catalyzed H_2O_2 oxidation: intermediate **5** is the active oxidant when Cit/HNO are formed from NOHA.

Influences of BH4 in Stage II. Whereas binding of BH4 is shown here to significantly accelerate the conversion of **5**/Arg to product, it slows conversion of **4**/NOHA to product, perhaps because of a decrease in the rate-limiting protonation of **4**/NOHA to form the **5**/NOHA at 160 K. Overall, these data show that BH4 affects the structure and reactivity of the intermediates along the reaction pathway, and that the cofactor effect is dependent on the substrate structure.

Cryoreduction and the Proton Delivery Network. The analysis of proton delivery presented above refers to reactions at temperatures below ~160 K, where mobility of protein residues and water(s) involved in the proton-delivery network is restricted. The finding that substrate quantitatively converts to product during cryoreduction/annealing necessarily requires that the enzyme has been cooled into a low-energy state (or ensemble of substates) in which the network is fully formed, including an H-bond between the proximate proton donor(s) and the peroxo/hydroperoxy ligand. Conversely, if the proton-transfer process is modified, as in the shunt variant of Stage II with hydrogen peroxide as oxidant, a mixture of the natural (citrulline) and alternative (cyanoornithine) products is observed.[17] Although one cannot rule out the operation of additional pathways at ambient temperatures, we suggest that protein thermal fluctuations introduced by warming from cryogenic to ambient temperatures are more likely to disrupt an already ordered pathway than they are to form a new one and that the cryoreduction studies, overall, faithfully represent the processes that occur under ambient conditions.

On the other hand, it is possible that a proton donor, such as a carboxyl group, cannot be "recharged" after giving up its proton at low temperature, whereas at ambient temperature, protein fluctuations might well enable the rapid reprotonation of a carboxylate from bulk solution. In addition, 77 K cryoreduction of **3**/Arg gives **5**/Arg directly, equivalent to a proton-coupled electron transfer, whereas **3**/NOHA gives **4**/NOHA,

(61) Abu-Soud, H. M.; Wu, C.; Ghosh, D. K.; Stuehr, D. J. *Biochemistry* **1998**, *37*, 3777–3786.
(62) Renodon, A.; Boucher, J.-L.; Wu, C.; Gachhui, R.; Sari, M.-A.; Mansuy, D.; Stuehr, D. *Biochemistry* **1998**, *37*, 6367–6374.
(63) Gerber, N. C.; Rodriguez-Crespo, I.; Nishida, C. R.; Ortiz de Montellano, P. R. *J. Biol. Chem.* **1997**, *272*, 6285–6290.
(64) Sorlie, M.; Gorren, A. C. F.; Marchal, S.; Shimizu, T.; Lange, R.; Andersson, K. K.; Mayer, B. *J. Biol. Chem.* **2003**, *278*, 48602–48610.
(65) Cho, K.-B.; Gauld, J. W. *J. Am. Chem. Soc.* **2004**, *126*, 10267–10270.
(66) Pufahl, R. A.; Wishnok, J. S.; Marletta, M. A. *Biochemistry* **1995**, *34*, 1930–1941.
(67) Fukuto, J. M. *Methods Enzymol.* **1996**, *268*, 365–375.

which subsequently acquires a proton. It may be that those two steps merge under physiological conditions.

Summary

Cryoreduction EPR/ENDOR measurements confirm that Compound I (**6**, Scheme 1) is the reactive heme species during the gsNOS-catalyzed Stage I oxidation of L-arginine to NOHA, whereas the active species during the Stage II oxidation of NOHA to citrulline and HNO/NO^- is **5**. Given the sensitivity of monooxygenase catalysis to active-site control and to the timing and mode of electron/proton delivery, it is important to emphasize the key correspondence between catalysis initiated by cryoreduction of **3** and that which proceeds upon one-electron reduction of **3** by BH4 under physiological conditions: in both cases, L-Arg is quantitatively hydroxylated to NOHA (Stage I), while NOHA is quantitatively converted to Cit and HNO (Stage II); when **3** is reduced by BH4 rather than an external reductant, the resulting BH4 radical oxidizes HNO/NO^- to produce NO as the final product.

The cryoreduction experiments further indicate that delivery of the first proton of catalysis to **4** in Stage I (Scheme 1) involves a bound water that conveys a proton from L-Arg, while the second proton likely derives from the carboxyl side chain of Glu 248 or a heme carboxylate group in a process that also involves proton delivery by water molecules. In the Stage II oxidation of NOHA, species **4**/NOHA trapped after cryoreduction is protonated to form **5**/NOHA, with the proton likely deriving from NOHA, a conclusion supported by the pH invariance of the process.

Of particular importance, the present results illustrate/support the idea that the substrate itself can modulate the monooxygenase reaction pathway, to the degree that different substrates react with different active enzyme states. We first demonstrated this substrate modulation in P450cam and its mutant T252A.[42] This concept is particularly well illustrated by NOS, as this one enzyme carries out its two physiologically important reaction steps with two different reactive heme species: the Cpd I heme in the hydroxylation of Arg and the ferric hydroperoxo heme during oxidation of NOHA. In part this difference may reflect the fact that NOHA is more reactive than L-Arg and thus is susceptible to attack by **5**. However, it also is likely that the mechanisms of the first and second half-reactions are different because the hydrogen-bonding/proton-delivery network in the active site is different with Arg and NOHA as substrate. We suggest that the modulation of the catalytically active heme-oxygen species by substrate is an important and general feature in the mechanisms of heme monooxygenases.

Acknowledgment. This work was supported by the NIH (HL13531, B.M.H.) and the NSF (CHE-0749997, B.R.C.).

Supporting Information Available: Figures S1−S13, showing EPR, ENDOR, and UV−vis spectra, HPLC traces, and time courses and kinetics of decays. This material is available free of charge via the Internet at http://pubs.acs.org.

JA906133H